Ministry of High Education

and Scientific Research

University of Babylon

College of Materials Engineering

Effect of The Loading Levels of Hydroxylamine and Sodium Carbonate on Adsorption Properties of y-FerOs: PAN Films

BY

Mustafa Hussain

Supervisor by

Dr.Salih Abbas

بسم الله الرحمن الرحيم

﴿يَرْفَعِ اللَّهُ الَّذِينَ آمَنُوا مِنْكُمْ وَالَّذِينَ أُوتُوا الْعِلْمَ دَرَجَاتٍ وَاللَّهُ بِمَا تَعْمَلُونَ خَبِيرٌ﴾

صدق الله العلي العظيم

" سورة المجادلة، آية: ١١."

الاهداء

الى الكهف الحصين وغياث المضطر المستكين وملاذ المؤمنين

إن حقوق إمامنا صاحب العصر والزمان أرواحنا فداه علينا كثيرة :

فهو العمود بين السماء والارض ...

اختم بحث تخرجي الى صاحب العصر والزمان والى كل من

ساندني في مسيرة الستّة عشر عاماً

داعي من اللَّهُ جَلَّ وَعَلاَ أن يوفقني ويوفق كل من سلك طريق العلم .

الشكر والتقدير

قال تعالى (وَمَنْ يَشْكُرْ فَإِنَّمَا يَشْكُرُ لِنَفْسِهِ) { لقمان :١٢ **}**

و قال رسوله الكريم صلوات الله عليه و اله : و من لم يشكر الناس ، لم يشكر الله عز و جل" . صدق رسول الله

احمد الله تعالى حمدا" طيبا" ملئ السماوات و الارض على ما اكرمني به من اتمام هذه الدراسة التي ارجو ان تنال رضاه .

ثم اوجه جزيل الشكر و عظيم الامتنان الى

الدكتور صالح عباس الجوذري . حفظه الله و اطال في عمره ، لتفظله الكريم بالاشراف على هذا البحث ، بنصحي و توجيهي حتى اتمام هذه الدراسة .

كما اوجه شكري الى جميع من في كلية هندسة المواد قسم هندسة البوليمرات و الصناعات البتروكمياوية جامعة بابل و الى كل من ساندني في هذه المسيرة العلمية .

Supervisor Certification:

We certify that this is these entitled (Effect of The Loading Levels of Hydroxylamine and Sodium Carbonate on Adsorption Properties of y-FerOs: PAN Films) was prepared

by "Mustafa Hussain Ayham" under our supervision at Babylon University of Material Engineering Department of Polymer and Petrochemical industries, in partial fulfillment of requirements for the Award Bachelor Degree of Science in Material Engineering Polymer and Petrochemical industries.

We Recommend that this thesis be forward for examinations in

accordance with the regulation of the University of Babylon.

Signature:

Supervisor Name: Dr.Salih Abbas.

Date: / /□□□□

Abstract

In this research, polyacrylonitrile nanofibers were prepared at a concentration of 12% by weight after dissolving them in a solvent N,N-dimethylformamide (DMF) and weight percentages (5, 8, 11% by weight of titanium oxide) were prepared, as well as the development of polyacrylonitrile by reacting a polyacrylonitrile solution with hydroxyl Amine hydrochloride and in the presence of sodium carbonate to produce amidoxime polyacrylonitrile (AOPAN) fibers. The produced fibers were examined by field emission scanning electron microscopy (FE-SEM), by X-ray diffraction (XRD), Fourier transform infrared (FT-IR) spectrophotometer, and by Differential scanning calorimetry-thermogravimetric analysis (DSC-TGA). Titanium oxide leads to a significant increase in the diameter of the nanofibers in addition to increasing the crystalline and thermal properties. The effect of titanium oxide on the developed polyacrylonitrile fibers (AOPAN), it will be less than in the case of adding it to the undeveloped polyacrylonitrile, as the fibers have better morphological and crystalline properties and thermal stability.

Table of Contents

Chapter One

1-Introduction

With the fast growth of industries worldwide and the advancement of new technologies, environmental contamination has posed a signifcant danger to both human health and ecosystem; particularly heavy metal ions amounts (e.g., The ions of Cd, Pb, Cr, Cu, Fe, Ni) in wastewater [1]. Heavy metal ions are non-degradable and always tend to aggregate in living organisms. Those metals are toxic even at relatively trace levels; consequently, this kind of pollution is damaging human health and the ecological system. Exposure to trace levels of lead and nickel adversely afect the human organs, brilliance, cardiovascular system, bone improvement, and the immune system. Moreover, lead may trigger brain disorders [2], while excessive intake of copper could cause liver and kidney failure [3]. Lead, copper, and nickel are found in many industries such as mining, metal electroplating, coating and painting, petrochemical, plumbing, and battery manufacturing [4, 5]. In the last few years, there have been considerable efforts development of treatment methods to remove metal ions from water, including chemical precipitation [6], membrane separation [7], solvent extraction [8], ion exchange [9], and adsorption [10]. Among these, adsorption is recognized as an effective method to remove heavy metal ions from aqueous systems [11]. Moreover, using polymer materials as an adsorbent that can be regenerated adds more advantages to adsorption over other methods. Electrospinning is considered as a straightforward and alterable technology to produce nanofibers adsorbents. The non-woven mats obtained from electrospun nanofbers display plenty of eye-opening characteristics such as high porosity, large surface area per unit mass, high gas permeability, and narrow distribution of pore size [10]. Many nanofbrous (NFs) adsorbents have been functionalized by electrospinning to remove metal ions [12–16]. Among these various functionalized polymers, Polyacrylonitrile (PAN) has demonstrated itself as an excellent polymer to be electrospun due to many advantages like easy processability, high chemical resistance, thermal stability, and excellent wettability with water [17]. Furthermore, the plenty amount of nitrile groups (C≡N) that exist abundantly on the surface of the PAN can be simply modifed into active functional groups through chemical reactions that can chelate heavy metal ions [18]. Up to date, the majority of work to convert the (C≡N) group into the amidoxime chelating group is done after PAN Electrospinning, but it still has some

drawbacks. First, when the neat nanofbers are being soaked, they might bend causing many shrinkages [10]. Besides, PAN NFs mats composed of many layers; consequently, the inner and outer fbers will have diferent degrees of amidoximation after being soaked [19]. In 2015 Xie et al. [20] came up with a methodology to synthesis excellent AOPAN mats to extract uranium from seawater. Ren et al. [19] synthesized nanofbers of AOPAN to sequester copper (II), lead (II) ions, \and dyes from aqueous media by electrospinning. Continuous-fow column type is more favoured over batch type and industrially viable since the rate of adsorption depends on the amount of ions in the solution being treated. In column type, the solution is in constant contact with the adsorbent and the concentration alters gradually, while in batch system, the amount of ions gets adsorbed abruptly, which adversely afects the adsorbent's efciency. Moreover, the continuous mode is easier and cheaper compared to the batch mode and can be simply scaled up from laboratory to industry [21].

1.2 Aim of the research

Preparation of polyacrylonitrile nanofibers reinforced with Titanium Isopropoxide, as well as the development of polyacrylonitrile by reacting the polyacrylonitrile solution with hydroxylamine hydrochloride and in the presence of sodium carbonate to produce Amidoxime Polyacrylonitrile (AOPAN) fibers and comparing the results of the two materials.

Chapter Two

i. THE THEORETICAL PART

2.1.0 Polyacrylonitrile (PAN)

also known as polyvinyl cyanide and Creslan 61, is a synthetic, semicrystalline organic polymer resin, with the linear formula (C3H3N)n. Though it is thermoplastic, it does not melt under normal conditions. It degrades before melting. It melts above 300 °C if the heating rates are 50 degrees per minute or above.[22] Almost all PAN resins are copolymers made from mixtures of monomers with acrylonitrile as the main monomer. It is a versatile polymer used to produce large variety of products including ultra filtration membranes, hollow fibers for reverse osmosis, fibers for textiles, and oxidized PAN fibers. PAN fibers are the chemical precursor of very high-quality carbon fiber. PAN is first thermally oxidized in air at 230 °C to form an oxidized PAN fiber and then carbonized above 1000 °C in inert atmosphere to make carbon fibers found in a variety of both high-tech and common daily applications such as civil and military aircraft primary and secondary structures, missiles, solid propellant rocket motors, pressure vessels, fishing rods, tennis rackets and bicycle frames. It is a component repeat unit in several important copolymers, such as styrene-acrylonitrile (SAN) and acrylonitrile butadiene styrene (ABS) plastic.

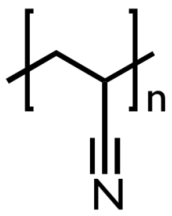

Taple 1

Names	
IUPAC name **poly(1-acrylonitrile)**	
Other names **Polyvinyl cyanide** **Creslan 61**	
Properties	
Chemical formula	**$(C_3H_3N)_n$**
Molar mass	**53.0626 ± 0.0028 g/mol** **C 67.91%, H 5.7%, N 26.4%**
Appearance	**White solid**
Density	**1.184 g/cm^3**
Melting point	**300 °C (572 °F; 573 K)**
Boiling point	**Degrades**
Solubility in water	**Insoluble**
Except where otherwise noted, data are given for materials in their standard state (at 25 °C [77 °F], 100 kPa).	

2.1.1 Applications

Homopolymers of polyacrylonitrile have been used as fibers in hot gas filtration systems, outdoor awnings, sails for yachts, and fiber-reinforced concrete. Copolymers containing polyacrylonitrile are often used as fibers to make knitted clothing like socks and sweaters, as well as outdoor products like tents and similar items. If the label of a piece of clothing says "acrylic", then it is made out of some copolymer of polyacrylonitrile. It was made into the spun fiber at DuPont in 1942 and marketed under the name of Orlon. Acrylonitrile is commonly employed as a comonomer with styrene, e.g. acrylonitrile, styrene and acrylate plastics. Labelling of items of clothing with acrylic (see acrylic fiber) means the polymer consists of at least 85% acrylonitrile as the monomer. A typical comonomer is vinyl acetate, which can be solution-spun readily to obtain fibers that soften enough to allow penetration by dyes. The advantages of the use of these acrylics are that they are low-cost compared to natural fiber, they offer better sunlight resistance and have superior resistance to attack by moths. Acrylics modified with halogen-containing comonomers are classified as modacrylics, which by definition contain more than PAN percentages between 35-85%. Incorporation of halogen groups increases the flame resistance of the fiber, which makes modacrylics suitable for the use in sleepwear, tents and blankets. However, the disadvantage of these products is that they are costly and can shrink after drying. PAN absorbs many metal ions and aids the application of absorption materials. Polymers containing amidoxime groups can be used for the treatment of metals because of the polymers' complex-forming capabilities with metal ions.[23] PAN has properties involving low density, thermal stability, high strength and modulus of elasticity. These

unique properties have made PAN an essential polymer in high tech. Its high tensile strength and tensile modulus are established by fiber sizing, coatings, production processes, and PAN's fiber chemistry. Its mechanical properties derived are important in composite structures for military and commercial aircraft [24].

- **Carbon fiber**

Polyacrylonitrile is used as the precursor for 90% of carbon fiber production. Approximately 20–25% of Boeing and Airbus wide-body airframes are carbon fibers. However, applications are limited by PAN's high price of around $15/lb [25,26] .

- **Glassy carbon**

Glassy carbon, a common electrode material in electrochemistry, is created by heat-treating blocks of polyacrylonitrile under pressure at 1000 to 3000 °C over a period of several days. The process removes non-carbon atoms and creates a conjugated double bond structure with excellent conductivity [27] .

- **Oxidized polyacrylonitrile fiber (OPF)**

Oxidized PAN Fiber is used to produce inherently flame resistant (FR) fabrics. Commonly when it is used in FR fabrics for protective apparel it is referred to as OPF (oxidized polyacrylonitrile fiber) and is a high-performance, cost-effective flame and heat resistance solution. OPF can be considered one of the most FR fabrics commercially produced since it has an LOI (Limiting Oxygen Index) in the range of 45–55% which is one of the highest LOI ranges available as compared with other common FR fabrics

which have lower LOI values (e.g. Nomex @ 28–30%, Kevlar @ 28–30%, Modacrylic @ 32–34%, PBI @ 41%, and FR-Viscose @ 28%);[citation needed] and OPF also demonstrates the lowest toxic gas generation upon burning as compared with other common fabrics (e.g. Nomex, FR Polyester, and Cotton) [28] .

- **Support polymer**

Polyacrylonitrile finds use as a porous supporting polymer for adsorbents for a variety of applications including ion exchange for cleaning up nuclear wastes. The PAN in this case is dissolved in a polar solvent such as DMSO along with the desired adsorbent and a surfactant and then dropped into water where it is crashed out and forms beads suitable for column use [28] .

- **Tholins**

Polyacrylonitrile is used in experiments as a precursor to tholin, a reddish-orange mixture of various organic compounds formed through radiolysis of carbon and nitrogen compounds. Naturally occurring tholins are expected to contain polyacrylonitrile and related heteropolymers containing some amino groups [26] .

2.2.0 Hydroxylammonium chloride

is a chemical compound with the formula [NH3OH]+Cl−. It is the hydrochloric acid salt of hydroxylamine (NH2OH). Hydroxylamine is a biological intermediate in nitrification (biological oxidation of ammonia with oxygen into nitrite) and in anammox (biological oxidation of nitrite and ammonium into dinitrogen gas) which are important in the nitrogen cycle in soil and in wastewater treatment plants[30,1].

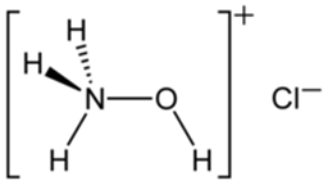

TABLE 2

Properties	
Chemical formula	[NH3OH]CI
Molar mass	69.49 g/mol
Appearance	white crystalline solid
Density	1.67 g/cm³
Melting point	155 to 157 °C (311 to 315 °F; 428 to 430 K) decomposes

[30,31].

2.2.1 Applications

Hydroxylammonium chloride is used in organic synthesis for preparation of oximes and hydroxamic acids from carboxylic acids, N- and O- substituted hydroxylamines, and addition reactions of carbon-carbon double bond. During the acetyl bromide method of extracting lignin from lignocellulosic biomass, hydroxylammonium chloride can be used to remove bromine and polybromide from the solution. In surface treatments, it is used in the preparation of anti-skinning agents, corrosion inhibitors, and cleaner additives. It is also a starting material for pharmaceuticals and agrochemicals manufacturing. In the rubber and plastics industries, it is an antioxidant, vulcanization accelerator, and radical scavenger. It is also used as a fixative for textile dyes, auxiliary in some dyeing processes, as a metal extraction and flotation aid, as an antioxidant in fatty acids and soaps, and as a color stabilizer and emulsion additive in color films. It is also used in analytic chemistry in the analysis of iron in the water combined with α,α-dipyridyl. The hydroxylammonium chloride transforms all the iron in Fe^{2+}, that then forms a coordination complex with the dipyridyl [30,31] .

2.3.0 Sodium carbonate

(also known as washing soda, soda ash and soda crystals) is the inorganic compound with the formula Na2CO3 and its various hydrates. All forms are white, odourless, water-soluble salts that yield alkaline solutions in water. Historically, it was extracted from the ashes of plants grown in sodium-rich soils. Because the ashes of these sodium-rich plants were noticeably different from ashes of wood (once used to produce potash), sodium carbonate became known as "soda ash". It is produced in large quantities from sodium chloride and limestone by the Solvay process, as well as by carbonating sodium hydroxide which is made using the Chlor-alkali process[39].

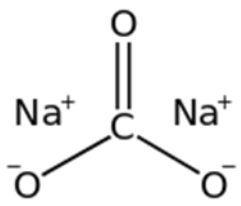

Table 3

Properties	
Chemical formula	Na_2CO_3
Molar mass	105.9888 g/mol (anhydrous) 286.1416 g/mol (decahydrate)
Appearance	White solid, hygroscopic
Odor	Odorless

Density	• 2.54 g/cm^3 (25 °C, anhydrous) • 1.92 g/cm^3 (856 °C) • 2.25 g/cm^3 (monohydrate)[32]. • 1.51 g/cm^3 (heptahydrate) • 1.46 g/cm^3 (decahydrate)[33].
Melting point	851 °C (1,564 °F; 1,124 K) (Anhydrous) 100 °C (212 °F; 373 K) decomposes (monohydrate) 33.5 °C (92.3 °F; 306.6 K) decomposes (heptahydrate) 34 °C (93 °F; 307 K) (decahydrate)[33,38].
Solubility in water	Anhydrous, g/100 mL: • 7 (0 °C) • 16.4 (15 °C) • 34.07 (27.8 °C) • 48.69 (34.8 °C) • 48.1 (41.9 °C) • 45.62 (60 °C)

	• 43.6 (100 °C)[34]
Solubility	Soluble in aq. alkalis,[34]. glycerol Slightly soluble in aq. alcohol Insoluble in CS_2, acetone, alkyl acetates, alcohol, benzonitrile, liquid ammonia[35].
Solubility in glycerine	98.3 g/100 g (155 °C)[35].
Solubility in ethanediol	3.46 g/100 g (20 °C)[36].
Solubility in dimethylformamide	0.5 g/kg[36].
Acidity (pK_a)	10.33 [37].
Magnetic susceptibility (χ)	$-4.1 \cdot 10^{-5}$ cm^3/mol[33].
Refractive index (n_D)	1.485 (anhydrous) 1.420 (monohydrate)[38]. 1.405 (decahydrate)
Viscosity	3.4 cP (887 °C)[36].

2.3.1 Applications

Some common applications of sodium carbonate include:

As a cleansing agent for domestic purposes like washing clothes. Sodium carbonate is a component of many dry soap powders. It has detergent properties through the process of saponification, which converts fats and grease to water-soluble salts (soaps, actually)[40].

It is used for lowering the hardness of water[41]. (see § Water softening).

It is used in the manufacture of glass, soap, and paper (see § Glass manufacture).

It is used in the manufacture of sodium compounds like borax.

- Glass manufacture

Sodium carbonate serves as a flux for silica (SiO2, melting point 1,713 °C), lowering the melting point of the mixture to something achievable without special materials. This "soda glass" is mildly water-soluble, so some calcium carbonate is added to the melt mixture to make the glass insoluble. Bottle and window glass ("soda-lime glass" with transistion temperature ~570 °C) is made by melting such mixtures of sodium carbonate, calcium carbonate, and silica sand (silicon dioxide (SiO2)). When these materials are heated, the carbonates release carbon dioxide. In this way, sodium carbonate is a source

of sodium oxide. Soda-lime glass has been the most common form of glass for centuries. It is also a key input for tableware glass manufacturing[40].

- Water softening

Hard water usually contains calcium or magnesium ions. Sodium carbonate is used for removing these ions and replacing them with sodium ions[41].

Sodium carbonate is a water-soluble source of carbonate. The calcium and magnesium ions form insoluble solid precipitates upon treatment with carbonate ions:

$Ca2+ + CO2{-}3 \rightarrow CaCO3\ (s)$

The water is softened because it no longer contains dissolved calcium ions and magnesium ions[41].

- Food additive and cooking

Sodium carbonate has several uses in cuisine, largely because it is a stronger base than baking soda (sodium bicarbonate) but weaker than lye (which may refer to sodium hydroxide or, less commonly, potassium hydroxide). Alkalinity affects gluten production in kneaded doughs, and also improves browning by reducing the temperature at which the Maillard reaction occurs. To take advantage of the former effect, sodium carbonate is therefore one of the components of kansui (かん水), a solution of alkaline salts used to give Japanese ramen noodles their characteristic flavor and chewy texture; a similar solution is used in Chinese cuisine to make lamian, for similar reasons. Cantonese bakers similarly use sodium carbonate as a substitute for lye-water to give moon cakes their characteristic texture and improve browning. In German cuisine (and Central European cuisine more broadly),

breads such as pretzels and lye rolls traditionally treated with lye to improve browning can be treated instead with sodium carbonate; sodium carbonate does not produce quite as strong a browning as lye, but is much safer and easier to work with. Sodium carbonate is used in the production of sherbet powder. The cooling and fizzing sensation results from the endothermic reaction between sodium carbonate and a weak acid, commonly citric acid, releasing carbon dioxide gas, which occurs when the sherbet is moistened by saliva. Sodium carbonate also finds use in food industry as a food additive (E500) as an acidity regulator, anticaking agent, raising agent, and stabilizer. It is also used in the production of snus to stabilize the pH of the final product. While it is less likely to cause chemical burns than lye, care must still be taken when working with sodium carbonate in the kitchen, as it is corrosive to aluminum cookware, utensils, and foil [42,43].

2.4.0 Dimethylformamide

is an organic compound with the formula (CH3)2NC(O)H. Commonly abbreviated as DMF (although this initialism is sometimes used for dimethylfuran, or dimethyl fumarate), this colourless liquid is miscible with water and the majority of organic liquids. DMF is a common solvent for chemical reactions. Dimethylformamide is odorless, but technical-grade or degraded samples often have a fishy smell due to impurity of dimethylamine. Dimethylamine degradation impurities can be removed by sparging samples with an inert gas such as argon or by sonicating the samples under reduced pressure. As its name indicates, it is structurally related to formamide, having two methyl groups in the place of the two hydrogens. DMF is a polar (hydrophilic) aprotic solvent with a high boiling point. It facilitates reactions that follow polar mechanisms, such as SN2 reactions.

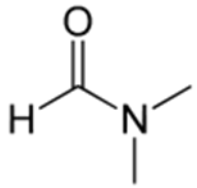

Table 4

Properties	
Chemical formula	C_3H_7NO
Molar mass	73.095 g·mol^{-1}

Appearance	Colourless liquid
Odor	Odorless, fishy if impure
Density	0.948 g/mL
Melting point	−61 °C (−78 °F; 212 K)
Boiling point	153 °C (307 °F; 426 K)
Solubility in water	Miscible
log *P*	−0.829
Vapor pressure	516 Pa
Acidity (pK_a)	-0.3 (for the conjugate acid) (H_2O)[44].
UV-vis (λ_{max})	270 nm
Absorbance	1.00
Refractive index (n_D)	1.4305 (at 20 °C)
Viscosity	0.92 mPa s (at 20 °C)

2.4.1 Applications

The primary use of DMF is as a solvent with low evaporation rate. DMF is used in the production of acrylic fibers and plastics. It is also used as a solvent in peptide coupling for pharmaceuticals, in the development and production of pesticides, and in the manufacture of adhesives, synthetic leathers, fibers, films, and surface coatings[45].

- It is used as a reagent in the Bouveault aldehyde synthesisand in the Vilsmeier-Haack reaction,[46][47] another useful method of forming aldehydes[48-50] .
- It is a common solvent in the Heck reaction[51].
- It is also a common catalyst used in the synthesis of acyl halides, in particular the synthesis of acyl chlorides from carboxylic acids using oxalyl or thionyl chloride. The catalytic mechanism entails reversible formation of an imidoyl chloride (also known as the 'Vilsmeier reagent'): [52,53].

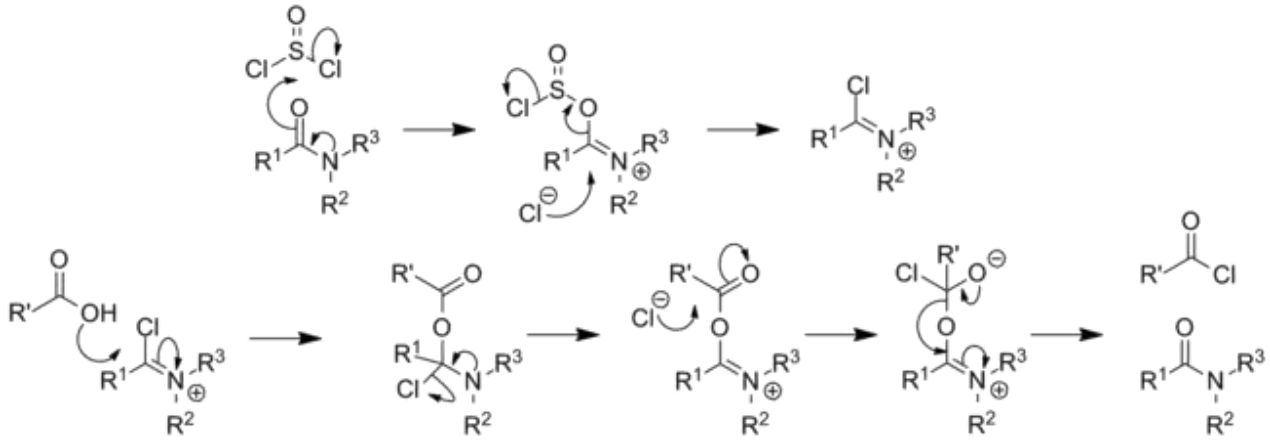

- DMF penetrates most plastics and makes them swell. Because of this property DMF is suitable for solid phase peptide synthesis and as a component of paint strippers.

- DMF is used as a solvent to recover olefins such as 1,3-butadiene via extractive distillation.
- It is also used in the manufacturing of solvent dyes as an important raw material. It is consumed during reaction.
- Pure acetylene gas cannot be compressed and stored without the danger of explosion. Industrial acetylene is safely compressed in the presence of dimethylformamide, which forms a safe, concentrated solution. The casing is also filled with agamassan, which renders it safe to transport and use.

As a cheap and common reagent, DMF has many uses in a research laboratory.

- DMF is effective at separating and suspending carbon nanotubes, and is recommended by the NIST for use in near infrared spectroscopy of such[54].
- DMF can be utilized as a standard in proton NMR spectroscopy allowing for a quantitative determination of an unknown compound.
- In the synthesis of organometallic compounds, it is used as a source of carbon monoxide ligands.
- DMF is a common solvent used in electrospinning.
- DMF is commonly used in the solvothermal synthesis of metal–organic frameworks.
- DMF-d_7 in the presence of a catalytic amount of KO*t*-Bu under microwave heating is a reagent for deuteration of polyaromatic hydrocarbons.

2.5.0 Electrospinning

is a fiber production method that uses electric force to draw charged threads of polymer solutions or polymer melts up to fiber diameters in the order of some hundred nanometers. Electrospinning shares characteristics of both electrospraying and conventional solution dry spinning of fibers[55]. The process does not require the use of coagulation chemistry or high temperatures to produce solid threads from solution. This makes the process particularly suited to the production of fibers using large and complex molecules. Electrospinning from molten precursors is also practiced; this method ensures that no solvent can be carried over into the final product.

2.5.1 Process

When a sufficiently high voltage is applied to a liquid droplet, the body of the liquid becomes charged, and electrostatic repulsion counteracts the surface tension and the droplet is stretched; at a critical point a stream of liquid erupts from the surface. This point of eruption is known as the Taylor cone. If the molecular cohesion of the liquid is sufficiently high, stream breakup does not occur (if it does, droplets are electrosprayed) and a charged liquid jet is formed [56,57] . As the jet dries in flight, the mode of current flow changes from ohmic to convective as the charge migrates to the surface of the fiber. The jet is then elongated by a whipping process caused by electrostatic repulsion initiated at small bends in the fiber, until it is finally deposited on the grounded collector. The elongation and thinning of the fiber resulting from this bending instability leads to the formation of uniform fibers with nanometer-scale diameters[58,59].

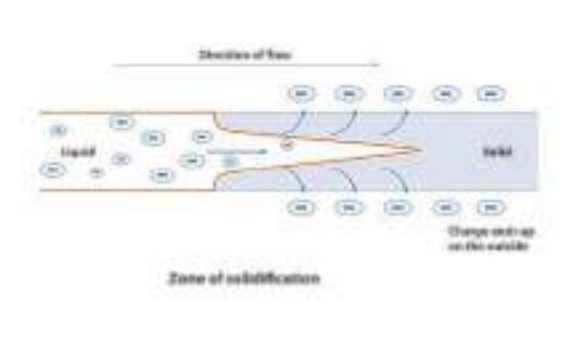

How the distribution of charge in the fibre changes as the fibre dries during flight

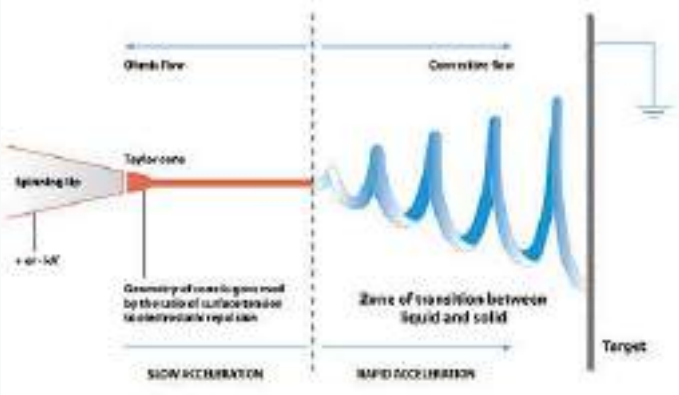

Diagram showing fibre formation by electrospinning

2.5.2 Parameters

- Molecular weight, molecular-weight distribution and architecture (branched, linear etc.) of the polymer
- Solution properties (viscosity, conductivity and surface tension)
- Electric potential, flow rate and concentration
- Distance between the capillary and collection screen
- Ambient parameters (temperature, humidity and air velocity in the chamber)
- Motion and size of target screen (collector)
- Needle gauge

Table 4

Effects of Electrospinning parameters.

Parameters	Effect on fibers	Linked to
	Solution Parameters	
Viscosity	If too low, no continuous fiber formation will occur; if too high, the ejection of the jet from the needle tip will be impeded.	*Polymer concentration, Molecular Weight*
Polymer Concentration	Increase in concentration results in increased diameter. A minimum concentration is required: if too low, there will not be enough entanglements to sustain the jet (*beads*).	*Surface tension, Viscosity*
Molecular weight	Reflects the number of *entanglements* of polymeric chains in solution, thus its viscosity.	*Viscosity, Surface tension, Conductivity*
Conductivity	Directly related to the accumulation of charges under the electric field. Higher conductivity results in stronger stretching of the jet producing smaller diameter fiber.	*Voltage*
Surface tension	With all other parameters fixed, it determines the upper and lower boundaries of the electrospinning window.	
	Processing Parameters	
Voltage	Fiber formation occurs only after a certain threshold voltage. Higher voltages cause greater stretching of the solution with reduction of fiber diameters; but if the voltage is too high, it may cause instability of the jet and increase the fiber	*Tip to collector distance, Conductivity, Feed rate*

	diameter.	
Tip to collector distance	Affects the traveling time of the polymer jet; should be high enough to allow complete evaporation of the solvent.	*Voltage, Feed rate*
Feed rate	Determines the amount of solution available per unit of time. Influences the jet velocity and the material transfer rate. Increasing the rate causes more polymer to be processed at a given instant, thus increasing fiber diameter.	*Tip to collector distance, Voltage, Viscosity*
	Ambient Parameters	
Humidity	High humidity may result in pores on fiber surface	
Temperature	An increase in temperature results in a decrease in fiber diameter thanks to a decrease in viscosity.	*Viscosity*

2.5.3 Apparatus and range

The standard laboratory setup for electrospinning consists of a spinneret (typically a hypodermic syringe needle) connected to a high-voltage (5 to 50 kV) direct current power supply, a syringe pump, and a grounded collector. A polymer solution, sol-gel, particulate suspension or melt is loaded into the syringe and this liquid is extruded from the needle tip at a constant rate by a syringe pump. Alternatively, the droplet at the tip of the spinneret can be replenished by feeding from a header tank providing a constant feed pressure. This constant pressure type feed works better for lower viscosity feedstocks[60].

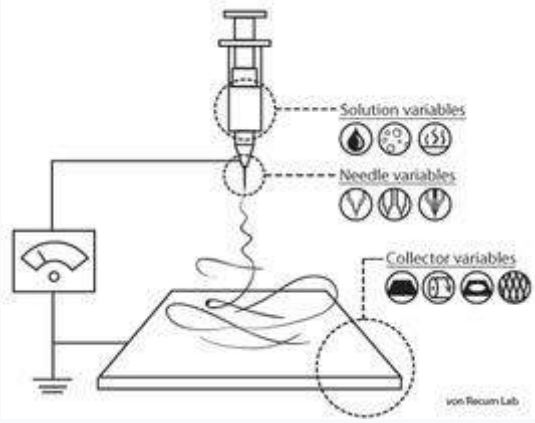

Electrospinning/electrospraying schematic with variations for different processing outcomes.

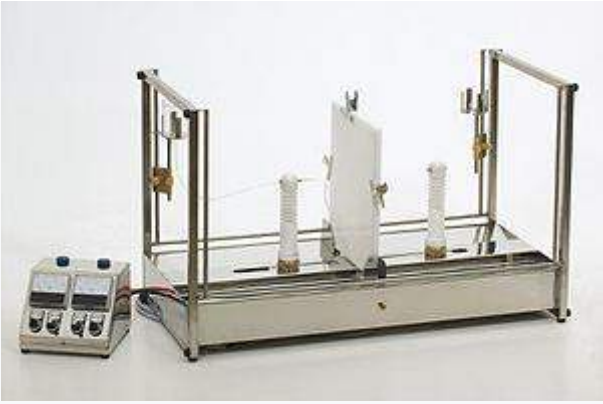

A constant pressure laboratory electrospinning machine (set up for horizontal fiber production)

2.5.4 Scaling-up possibilities

- Alternating current electrospinning [61-66].
- Needleless (also known as, nozzle-free) electrospinning [67,68].
- Multiplying the needles[69].
- High-throughput roller electrospinning][70].
- Wire electrospinning
- Bubble electrospinning[71].
- Ball electrospinning
- High speed electrospinning[72].
- Plate edge electrospinning[73].
- Bowl electrospinning[74].
- Hollow tube electrospinning[75].
- Rotary cone electrospinning[76].
- Spiral coil electrospinning[77].
- Electroblowing[78].

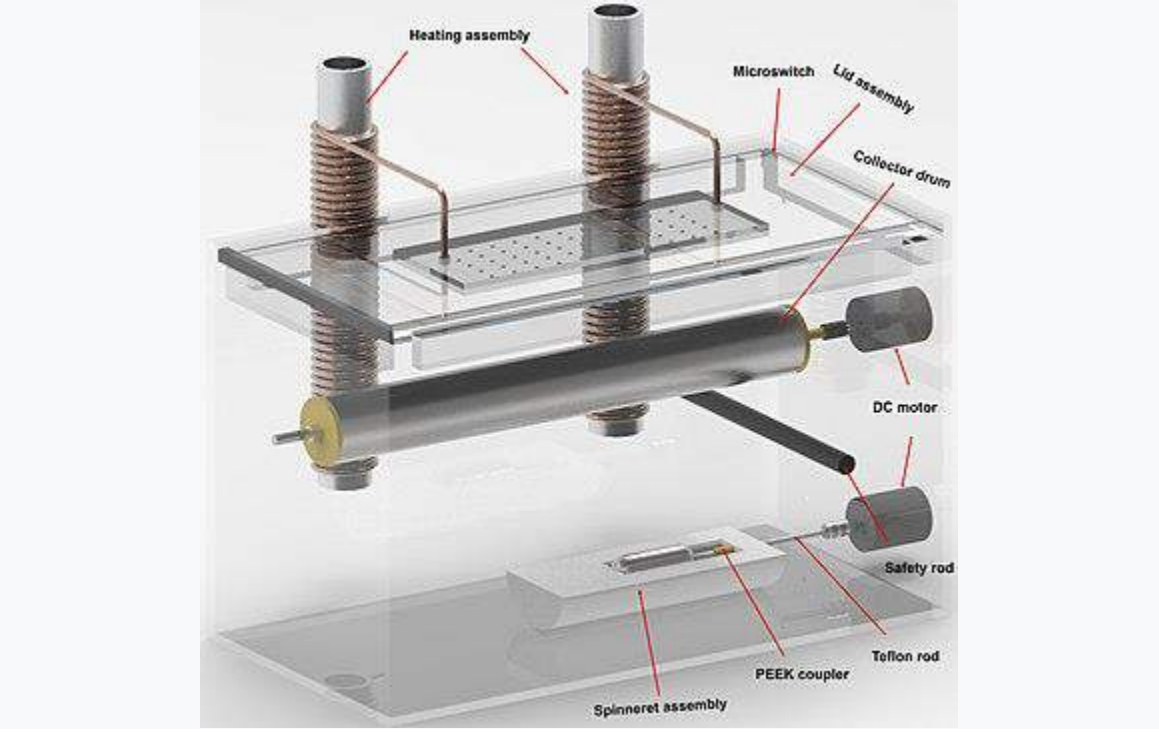

Schematic of an upward needleless roller electrospinning device. The setup comprises two oppositely charged rotating mandrels. A reservoir is used to finely coat the surface of the rotating spinneret (half-submerged, bottom mandrel) with a polymer solution layer. High-voltage is applied between the two mandrels, instigating the subsequent generation of fibers from the spinneret's surface. Due to the wider surface of the spinneret, high-throughput production is feasible [70].

2.5.5 Uses

The size of an electrospun fiber can be in the nano scale and the fibers may possess nano scale surface texture, leading to different modes of interaction with other materials compared with macroscale materials[82]. In addition to this, the ultra-fine fibers produced by electrospinning are expected to have two main properties, a very high surface to volume ratio, and a relatively defect free structure at the molecular level. This first property makes electrospun material suitable for activities requiring a high degree of physical contact, such

as providing sites for chemical reactions, or the capture of small sized particulate material by physical entanglement – filtration. The second property should allow electrospun fibers to approach the theoretical maximum strength of the spun material, opening up the possibility of making high mechanical performance composite materials.

i. Filtration

Lycopodium club moss spores (diameter about 60 micrometers) captured on an electrospun polyvinyl alcohol fiber

The use of nanofiber webs as a filtering medium is well established. Due to the small size of the fibers London-Van Der Waals forces are an important method of adhesion between the fibers and the captured materials. Polymeric nanofibers have been used in air filtration applications for more than seven decades[81,83] . Because of poor bulk mechanical properties of thin nanowebs, they are laid over a filtration medium substrate. The small fiber diameters cause slip flows at fiber surfaces, causing an increase in the interception and inertial impaction efficiencies of these composite filter media. The enhanced filtration efficiency at the same pressure drop is possible with fibers having diameters less than 0.5 micrometer. Since the essential properties of protective clothing are high moisture vapor transport, increased fabric breath-ability, and enhanced toxic chemical resistance,

electrospun nanofiber membranes are good candidates for these applications[84].

ii. Textile manufacturing

The majority of early patents for electrospinning were for textile applications, however little woven fabric was actually produced, perhaps due to difficulties in handling the barely visible fibers. However, electrospinning has the potential to produce seamless non-woven garments by integrating advanced manufacturing with fiber electrospinning. This would introduce multi-functionality (flame, chemical, environmental protection) by blending fibers into electrospinlaced (using electrospinning to combine different fibers and coatings to form three-dimensional shapes, such as clothing) layers in combination with polymer coatings[85,86].

iii. Medical

Electrospinning can also be used for medical purposes[87]. The electrospun scaffolds made for tissue engineering applications can be penetrated with cells to treat or replace biological targets[88]. Nanofibrous wound dressings [89]. have excellent capability to isolate the wound from microbial infections[90,91]. Other medical textile materials such as sutures are also attainable via electrospinning[92]. Through the addition of a drug substance into the electrospinning solution or melt [80]. diverse fibrous drug delivery systems (e.g., implants, transdermal patches, oral forms) [93-95]. can be prepared. Interestingly, electrospinning allows to fabricate nanofibers with advanced architecture that can be used to promote the delivery of multiple drugs at the same time and with different kinetics[96-98] .

iv. Cosmetic

Electrospun nanomaterials have been employed to control their delivery so they can work within skin to improve its appearance Electrospinning is an alternative to traditional nanoemulsions and nanoliposomes[99].

v. Pharmaceutical manufacturing

The continuous manner and the effective drying effect enable the integration of electrospinning into continuous pharmaceutical manufacturing systems The synthesized liquid drug can be quickly turned into an electrospun solid product processable for tableting and other dosage forms[100].

vi. Composites

Ultra-fine electrospun fibers show clear potential for the manufacture of long fiber composite materials[101].

Application is limited by difficulties in making sufficient quantities of fiber to make substantial large scale articles in a reasonable time scale. For this reason medical applications requiring relatively small amounts of fiber are a popular area of application for electrospun fiber reinforced materials.

Electrospinning is being investigated as a source of cost-effective, easy to manufacture wound dressings, medical implants, and scaffolds for the production of artificial human tissues. These scaffolds fulfill a similar purpose as the extracellular matrix in natural tissue. Biodegradable polymers, such as polycaprolactone and polysaccharides, are typically used for this purpose. These fibers may then be coated with collagen to promote cell attachment, although collagen has successfully been spun directly into membranes [102-104] .

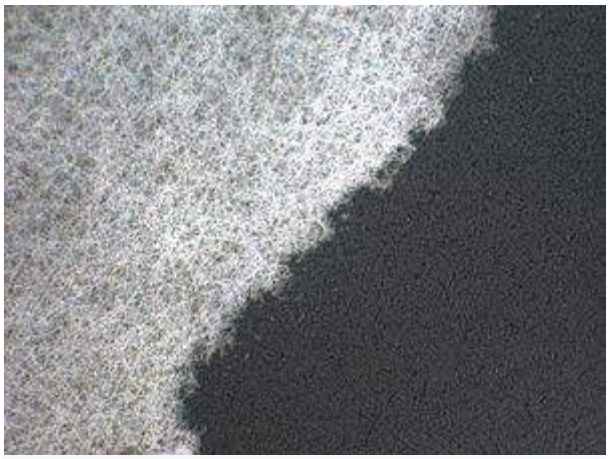

Optical image of epoxy resin impregnating an electrospun polyvinyl alcohol reinforcing fiber mat

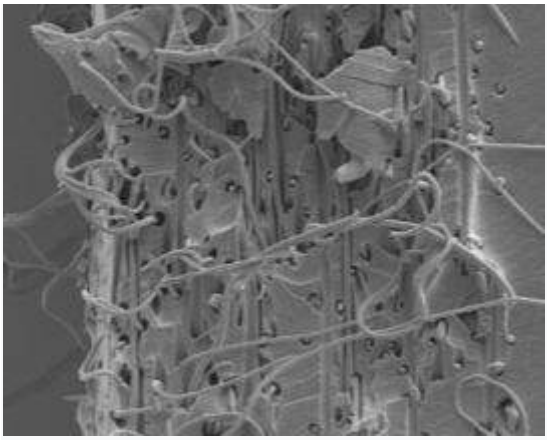

SEM image of the fracture surface of a polyvinyl alcohol long fiber – epoxy matrix composite – the section thickness is about 12 micrometers

vii. Catalysts

Electrospun fibers may have potential as a surface for enzymes to be immobilized on. These enzymes could be used to break down toxic chemicals in the environment, among other things[59] .

viii. Mass production

Thus far, at least eight countries in the world have companies which provide industrial-level and laboratory-scale electrospinning machines: three companies each in Italy and Czech Republic, two each in Iran, Japan, and Spain, and one each in the Netherlands, New Zealand and Turkey [105,106].

Chapter Three

3. Experimental Work

3.1. Materials

Polyacrylonitrile powder (PAN, MW = 150,000 g/mol) was purchased from Sigma–Aldrich, USA. Solvents, such as N,N-dimethylformamide (DMF) was purchased from Shanghai Chemical Reagents Co., Ltd, China and Ethanol with molar mass: 46.07 g/mol was purchased from Merck KGaA, Darmstadt, Germany . Titanium (IV) isopropoxide 97% and Hydroxylamine hydrochloride with molecular weight 69.49 g/ mol were purchased from Sigma–Aldrich, USA respectively. Sodium carbonate with molecular weight 105.99 g/mol was purchased from Merck KGaA, Darmstadt, Germany.

3.2 Preparation of Electrospinning Solutions

1. Titanium Isopropoxide-Polyacrylonitrile

Dissolve 12% (w/w) polyacrylonitrile powder in DMF solvent at a temperature not exceeding 40°C. Mixing will be done using a magnetic stirrer until homogeneity is achieved. Dilute the concentrated solution of Titanium isopropoxide (TiPP) with ethanol to three concentrations levels 5,8, and 11(w/w) % at a mixing ratio (7:3 TiPP: Ethanol) , then add a solution of TiPP: Ethanol to PAN :DMF solution drop by drop until a yellow homogeneous solution is obtained according to the details of electrospinning solutions composition in Table 1.

2. Amidoxime Polyacrylonitrile (AOPAN).

22.5 (w/w) % of the hydroxylamine hydrochloride was added to a 12% PAN: DMF solution at room temperature for 4 hours, followed by the addition of 17 (w/w) % of sodium carbonate to a polymer solution at a temperature not exceeding 70 °C for 3 hours based on the weight of the polymer to obtain the AOPAN solution, then the solution was left to cool after being filtered from insoluble materials [106]. The chemical reaction required to convert PAN to AOPAN takes place according to Scheme 1 [106].

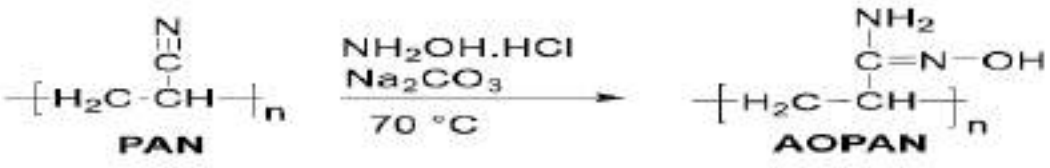

Scheme.1 Reaction of hydroxylamine hydrochloride with PAN nitrile group

Table 1 compositions of amidoxime polyacrylonitrile (AOPAN) and titanium isopropoxide-polyacrylonitrile (TiPP @PAN) electrospun solutions.

Samples	Polymers % (w/w)	TiPP % (w/w)	Ethanol % (w/w)	DMF % (w/w)
Pure PAN	12	-	-	88
5 % TiPP @PAN	12	5	2.14	80.86
8 % TiPP @PAN	12	8	3.43	76.57
11 % TiPP @PAN	12	11	4.71	72.29
AOPAN	16.7	-	-	83.30
5 % TiPP @AOPAN	16.7	5	2.14	76.16

(TiPP: Ethanol = 7:3) for all samples

The electrospinning process for all polymeric solutions is carried out with (1 mL / hr.) feed rate for the 1mL of syringe pump at room temperature and humidity not exceeding 40%, an electric

3.3.0 Examination devices

3.3.1.0 XRD

X-Ray Diffraction Testing & Analysis (XRD) Ray Diffraction Analysis is important to investigate crystalline material structure as well as atomic arrangement, crystallite size and imperfections. It is pivotal for the safety and efficacy of products. XRD is a valuable tool for analysis and testing of materials used in pharmaceuticals, food, cosmetics, studies in nanomaterials, blood, forensics, geological grading of minerals, electronics etc [106] .

XRD Analysis in the Pharmaceutical Industry

XRD Analysis in Food Industry

XRD Analysis in Cosmetics Industry

3.3.1.1 Manufacturing Process Control

• Measure the average spacings between

layers or rows of atoms

• Determine the orientation of a single

crystal or grain

• Find the crystal structure of an unknown

material

• Measure the size, shape and internal

stress of small crystalline regions

3.3.1.2 Applications of XRD

• XRD is a nondestructive technique

• To identify crystalline phases and orientation

• To determine structural properties:

Lattice parameters (10-4Å), strain, grain size,

expitaxy, phase composition, preferred orientation

(Laue) order-disorder transformation, thermal

expansion

• To measure thickness of thin films and multi-layers*

• To determine atomic arrangement

• Detection limits: ~3% in a two phase mixture; can be

~0.1% with synchrotron radiation

Spatial resolution: normally none

One of the most important uses of XRD!

• Obtain XRD pattern

• Measure d-spacings

• Obtain integrated intensities

• Compare data with known standards in the

JCPDS file, which are for random orientations

(there are more than 50,000 JCPDS cards of

inorganic materials) [106].

3.3.2.0 FE-SEM

Field Emission Scanning Electron Microscopy (FESEM) Field emission scanning electron microscopy (FESEM) provides topographical and elemental information at magnifications of 10x to 300,000x, with virtually unlimited depth of field. Compared with convention scanning electron microscopy (SEM), field emission SEM (FESEM) produces clearer, less electrostatically

distorted images with spatial resolution down to 1 1/2 nanometers – three to six times better [107] .

3.3.2.1 Other advantages of FESEM include

The ability to examine smaller-area contamination spots at electron accelerating voltages compatible with energy dispersive spectroscopy (EDS) Reduced penetration of low-kinetic-energy electrons probes closer to the immediate material surface. High-quality, low-voltage images with negligible electrical charging of samples (accelerating voltages ranging from 0.5 to 30 kilovolts) Essentially no need for placing conducting coatings on insulating materials. For ultra-high-magnification imaging, we use in-lens FESEM.

3.3.2.2 Applications of FESEM

Semiconductor device cross section analyses for gate widths, gate oxides, film thicknesses, and construction details Advanced coating thickness and structure uniformity determination Small contamination feature geometry and elemental composition measurement Principle of Operation A field-emission cathode in the electron gun of a scanning electron microscope provides narrower probing beams at low as well as high electron energy, resulting in both improved spatial resolution and minimized sample charging and damage. For applications that demand the highest magnification possible, we also offer in-lens FESEM [107] .

3.3.3.0 DSC

Differential scanning calorimetry (DSC) measures temperatures and heat flows associated with thermal transitions in a material. In this thermoanalytical technique, the difference in the amount of heat required to increase the temperatures of a sample and a reference are measured as a function of temperature. Both the sample and the reference are maintained at nearly the same temperature throughout the experiment. Generally, the temperature program for a DSC analysis is designed such that the sample holder temperature increases linearly as a function of time. Only a few milligrams of material are required to run the analysis [108].

3.3.3.1 Applications

Common usages of DSC include investigation, selection, comparison, and end-use performance evaluation of materials in research, quality control, and production applications. DSC is commonly used to measure a variety of properties in both organic and inorganic materials, from metals and simple compounds to polymers and pharmaceuticals. The properties measured include:

Glass transitions

Phase changes

Melting

Crystallization

Product stability

Cure/cure kinetics

Oxidative stability

Heat capacity and heat of fusion measurements

Principle of Operation

When a sample undergoes a physical transformation, such as a phase transition, more or less heat will need to flow to it than to the reference (typically an empty sample pan) to maintain both at the same temperature. Whether more or less heat must flow to the sample depends on whether the process is exothermic or endothermic.

For example, as a solid sample melts to a liquid, the sample will require more heat than the reference to increase its temperature at the same rate as the reference due to the absorption of heat by the sample as it undergoes the endothermic phase transition from solid to liquid. Likewise, as a sample undergoes exothermic processes (such as crystallization), the sample requires less heat than the reference to raise the sample temperature at the same rate as the reference. By observing the difference in heat flow between the sample and reference, differential scanning calorimeters can measure the amount of heat absorbed or released during such transitions. DSC may also be used to observe more-subtle phase changes, such as glass transitions [108] .

3.3.4.0 TGA

Thermogravimetric analysis (TGA) measures weight changes in a material as a function of temperature (or time) under a controlled atmosphere. Its principle uses include measurement of a material's thermal stability, filler content in polymers, moisture and solvent content, and the percent composition of components in a compound [109].

3.3.4.1 Applications

Principle uses of TGA include measurement of a material's thermal stability and its composition Typical applications inclue

Filler content of polymer resins

Residual solvent content

Carbon black content

Decomposition temperature

Moisture content of organic and inorganic materials

Plasticizer content of polymers

Oxidative stability

Performance of stabilizers

Low molecular weight monomers in polymers

Principle of Operation

A TGA analysis is performed by gradually raising the temperature of a sample in a furnace as its weight is measured on an analytical balance that remains outside of the furnace. In TGA, mass loss is observed if a thermal event involves loss of a volatile component. Chemical reactions, such as combustion, involve mass losses, whereas physical changes, such as melting, do not. The weight of the sample is plotted against temperature or time to illustrate thermal transitions in the material – such as loss of solvent and plasticizers in polymers, water of hydration in inorganic materials, and, finally, decomposition of the material[109].

3.3.5.0 FTIR

Fourier Transform Infrared (FTIR) Spectroscopy is used to perform qualitative and quantitative analysis of organic compounds and to determines the chemical structure of many inorganic compounds. The FTIR microscope accessory permits analysis of samples as small as a few microns in diameter. Shown is the new Agilent Cary 670 FTIR with the Cary 610 FTIR microscope recently acquired by PhotoMetrics.

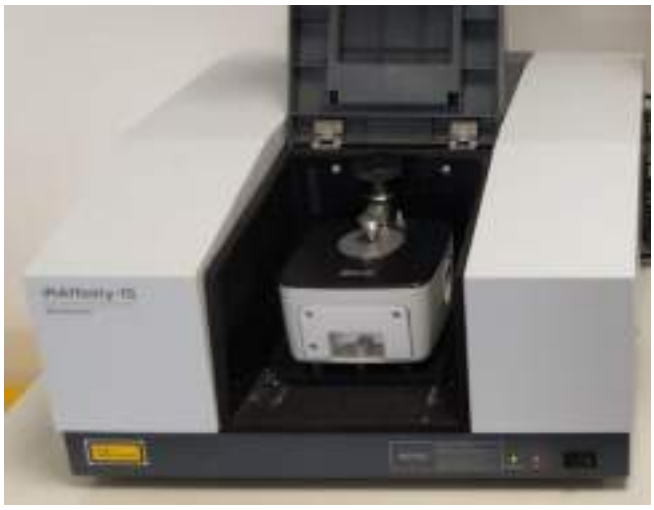

3.3.5.1 Applications

Materials evaluation and identification

Organic compounds

Structure of many inorganic compounds

Deformulations

Forensics

Material homogeneity

Principle of Operation Because chemical bonds absorb infrared (IR) energy at specific frequencies (wavelengths), the basic structure of compounds can be determined by the spectral locations of their IR absorptions. The plot of a compound's IR transmission versus frequency is its "fingerprint," which when compared to reference spectra identifies the material. PhotoMetrics maintains one of the largest commercial IR-spectrum libraries and offers a spectral search service to its industrial clients and other laboratories for identifying the materials in the spectra obtained. FTIR spectrometers offer speed and sensitivity that was impossible to achieve with earlier wavelength-dispersive instruments. This capability allows rapid analysis of micro samples down to the nanogram level in some cases, making the FTIR unmatched as a problem-solving tool in organic analysis. The FTIR microscope accessory allows spectra from a few nanograms of material to be obtained quickly, with little sample preparation, resulting in more data at lower cost. In some cases, thin films of residue are identified with a sensitivity that rivals or even exceeds surface analysis techniques based on electron or ion beams. As an analytical technique, FTIR has few sample constraints. Solids, liquids and gases can be accommodated. In addition, many contaminants present on reflective surfaces, such as solder pads or printed circuitry, are readily analyzed in situ using the FTIR microscope in reflectance mode [110].

3.3.6.0 EDX

Energy-dispersive X-ray spectroscopy (EDS, EDX, EDXS or XEDS), sometimes called energy dispersive X-ray analysis (EDXA or EDAX) or energy dispersive X-ray microanalysis (EDXMA), is an analytical technique used for the elemental analysis or chemical characterization of a sample. It relies on an interaction of some source of X-ray excitation and a sample. Its characterization capabilities are due in large part to the fundamental principle that each element has a unique atomic structure allowing a unique set of peaks on its electromagnetic emission spectrum (which is the main principle of spectroscopy). The peak positions are predicted by the Moseley's law with accuracy much better than experimental resolution of a typical EDX instrument. To stimulate the emission of characteristic X-rays from a specimen a beam of electrons is focused into the sample being studied. At rest, an atom within the sample contains ground state (or unexcited) electrons in discrete energy levels or electron shells bound to the nucleus. The

incident beam may excite an electron in an inner shell, ejecting it from the shell while creating an electron hole where the electron was. An electron from an outer, higher-energy shell then fills the hole, and the difference in energy between the higher-energy shell and the lower energy shell may be released in the form of an X-ray. The number and energy of the X-rays emitted from a specimen can be measured by an energy-dispersive spectrometer. As the energies of the X-rays are characteristic of the difference in energy between the two shells and of the atomic structure of the emitting element, EDS allows the elemental composition of the specimen to be measured.

3.3.6.1 Equipment

Four primary components of the EDS setup are

the excitation source (electron beam or x-ray beam)

the X-ray detector

the pulse processor

the analyzer.

Electron beam excitation is used in electron microscopes, scanning electron microscopes (SEM) and scanning transmission electron microscopes (STEM). X-ray beam excitation is used in X-ray fluorescence (XRF) spectrometers. A detector is used to convert X-ray energy into voltage signals; this information is sent to a pulse processor, which measures the signals and passes them onto an analyzer for data display and analysis. The most common detector used to be a Si(Li) detector cooled to cryogenic temperatures with liquid nitrogen. Now, newer systems are often equipped with silicon drift detectors (SDD) with Peltier cooling systems.

Technological variants

3.3.6.2 Principle of EDS

The excess energy of the electron that migrates to an inner shell to fill the newly created hole can do more than emit an X-ray. Often, instead of X-ray emission, the excess energy is transferred to a third electron from a further outer shell, prompting its ejection. This ejected species is called an Auger electron, and the method for its analysis is known as Auger electron spectroscopy (AES) [111].

X-ray photoelectron spectroscopy (XPS) is another close relative of EDS, utilizing ejected electrons in a manner similar to that of AES. Information on the quantity and kinetic energy of ejected electrons is used to determine the binding energy of these now-liberated electrons, which is element-specific and allows chemical characterization of a sample[111].

EDS is often contrasted with its spectroscopic counterpart, wavelength dispersive X-ray spectroscopy (WDS). WDS differs from EDS in that it uses the diffraction of X-rays on special

crystals to separate its raw data into spectral components (wavelengths). WDS has a much finer spectral resolution than EDS. WDS also avoids the problems associated with artifacts in EDS (false peaks, noise from the amplifiers, and microphonics).

A high-energy beam of charged particles such as electrons or protons can be used to excite a sample rather than X-rays. This is called particle-induced X-ray emission or PIXE.

Accuracy of EDS

EDS can be used to determine which chemical elements are present in a sample, and can be used to estimate their relative abundance. EDS also helps to measure multi-layer coating thickness of metallic coatings and analysis of various alloys. The accuracy of this quantitative analysis of sample composition is affected by various factors. Many elements will have overlapping X-ray emission peaks (e.g., Ti Kβ and V Kα, Mn Kβ and Fe Kα). The accuracy of the measured composition is also affected by the nature of the sample. X-rays are generated by any atom in the sample that is sufficiently excited by the incoming beam. These X-rays are emitted in all directions (isotropically), and so they may not all escape the sample. The likelihood of an X-ray escaping the specimen, and thus being available to detect and measure, depends on the energy of the X-ray and the composition, amount, and density of material it has to pass through to reach the detector. Because of this X-ray absorption effect and similar effects, accurate estimation of the sample composition from the measured X-ray emission spectrum requires the application of quantitative correction procedures, which are sometimes referred to as matrix corrections.

Emerging technology[111]

There is a trend towards a newer EDS detector, called the silicon drift detector (SDD). The SDD consists of a high-resistivity silicon chip where electrons are driven to a small collecting anode. The advantage lies in the extremely low capacitance of this anode, thereby utilizing shorter processing times and allowing very high throughput. Benefits of the SDD include:

High count rates and processing,

Better resolution than traditional Si(Li) detectors at high count rates,

Lower dead time (time spent on processing X-ray event),

Faster analytical capabilities and more precise X-ray maps or particle data collected in seconds,

Ability to be stored and operated at relatively high temperatures, eliminating the need for liquid nitrogen cooling.

Because the capacitance of the SDD chip is independent of the active area of the detector, much larger SDD chips can be utilized (40 mm^2 or more). This allows for even higher count rate collection. Further benefits of large area chips include:

Minimizing SEM beam current allowing for optimization of imaging under analytical conditions,

Reduced sample damage and

Smaller beam interaction and improved spatial resolution for high speed maps [111] .

3.4.0 specification of Material

3.4.1 polyacrylonitrile

diameter: 13±1um	**titer: 1.90±0.2detx**
length: 4-50mm	**density: 1.18g/cm3**
color: yellowish	**crack elongation: 15%±5%**
original modulus: ≥10.0Gpa	**tensile strength: ≥ 800Mpa**
acid-resistance: Excellent	**alkali-resistance: Excellent**

[112].

3.4.2 HYDROXYLAMINE HYDROCHLORIDE

VAPOR PRESSURE	**0.054 PA (50 °C)**
ASSAY	**≥96%**
FORM	**CRYSTALS**
PH	**2.5-3.5 (20 °C, 50 G/L IN H2O)**
MP	**154 °C**

SOLUBILITY	470 G/L
DENSITY	1.7 G/CM3 AT 20.2 °C
SHIPPED IN	AMBIENT
STORAGE TEMP.	ROOM TEMP
INCHI	1S/CLH.H3NO/C;1-2/H1H;2H,1H2

[113].

3.4.3SODIUM CARBONATE

Na_2CO_3	%	99.5 min
Na_2O	%	58.2 min
NaCl	%	0.1 max
Na_2SO_4	%	0.1 max
Total Fe	µg/g	10 max
Water Insolubles	%	0.05 max
As / Arsenic	ppm	1 max
Pb / Lead	ppm	1 max
Hg / Mercury	ppm	1 max
Solubility	g/100 ml water	45.5 (100°C) 49.5 (35.37 °C) 7 (0 °C)
pH	1 % solution	11.4

[114].

3.4.5 DMF

Properties	
Chemical formula	**C_3H_7NO**
Molar mass	**73.095 g·mol^{-1}**
Appearance	**Colourless liquid**
Odor	**Odorless, fishy if impure**
Density	**0.948 g/mL**
Melting point	**−61 °C (−78 °F; 212 K)**
Boiling point	**153 °C (307 °F; 426 K)**
Solubility in water	**Miscible**
log *P*	**−0.829**
Vapor pressure	**516 Pa**
Acidity (pK_a)	**-0.3 (for the conjugate**

	acid) (H_2O)
UV-vis (λ_{max})	**270 nm**
Absorbance	**1.00**
Refractive index (n_D)	**1.4305 (at 20 °C)**
Viscosity	**0.92 mPa s (at 20 °C)**

[53 ,54].

Chapter Four

4. Results and Discussion

4.1 Morphological Properties

Figure 1. FE-SEM images and histograms of nanofiber diameters for (A) Pure PAN, (B) 5% TiPPPAN, (C) 8% TiPPPAN, (D) 11% TiPPPAN, (E) AOPAN, and (F) 5% TiPPAOPAN, where the diameter of the nanofibers increases with increasing the added weight ratios of TiPP to PAN from 370 ± 126 nm to 1192.76 ± 440.63 nm when increased the TiPP wt.% from 5 wt.% to 11wt.% 341 ± 69 nm to 463 ± 109 nm after adding 5 wt.% of TiPP to AOPAN ,while the nanofiber diameter increased after added the 5 wt.% of TiPP to PAN from 244.37±126 nm to 370±126 nm.

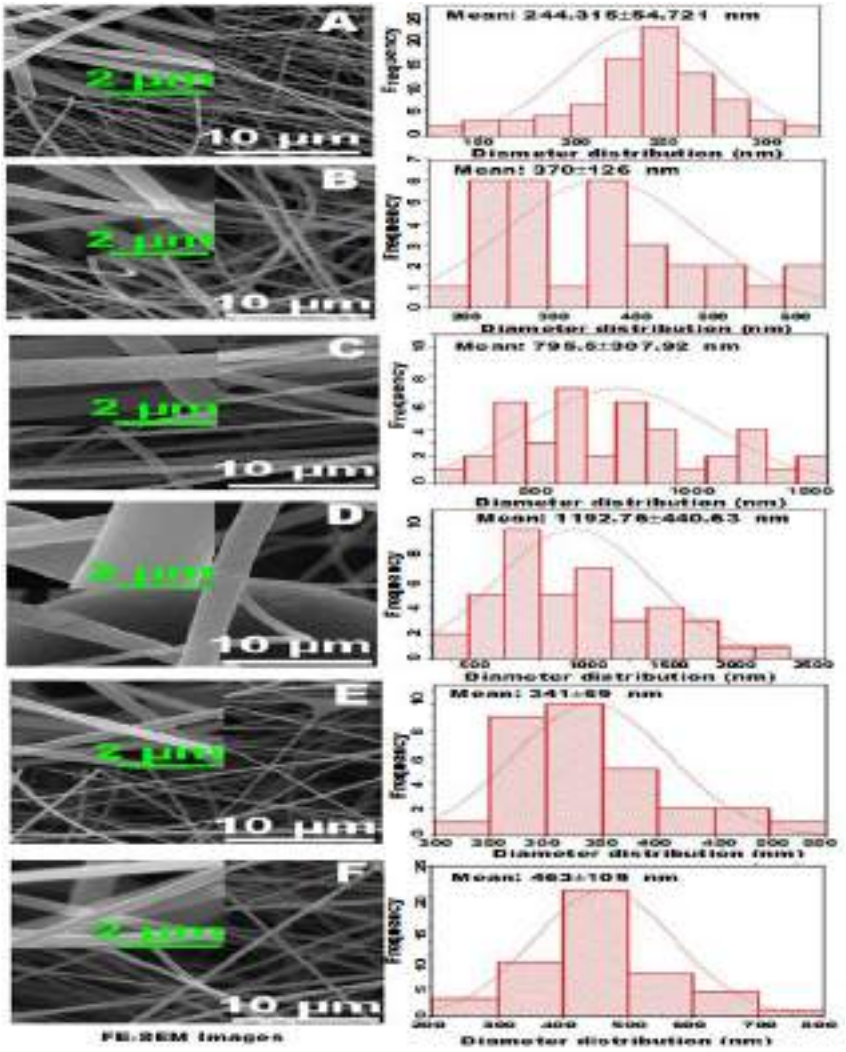

Figure 1 FE-SEM images and nanofiber diameters histograms of (A) Pure PAN , (B) 5 % TiPP @PAN , (C) 8 % TiPP @PAN , (D) 11 % TiPP @PAN , (E) AOPAN , and (F) 5 % TiPP @AOPAN respectively

4.2 FT-IR Analysis

Figure 2 shows the FT-IR spectra of pure of PAN, TiPP @ PAN, AOPAN, and TiPP@ AOPAN respectively. Figure 2A presents the FTIR spectra of pure PAN, where peaks 2243, 1740, and 1236 cm^{-1} represent (-CN) , (C=O), and (C-O) of these peaks and are attributed to PAN, as this copolymer is of methyl acrylate and acrylonitrile, peak 2243 cm^{-1} represents the nitrile group, which contributes to the partial conversion to amidoxime groups . On the other hand, for the reinforcement of PAN nanofibers by TiPP the peak 1625 cm^{-1} is attributed to the deformation vibrations of hydroxyl (–OH) and water (H2O) at the surface TiPP corresponding to Ti-OH group (Figure 2b)], also the absorption peaks from 469 corresponding to T i-O in TiPP [118-119].

While the Figure 2c presents the FTIR spectra of AOPAN. While the new bands appear at 1118 and 1669 stretching vibration of C–N and C=N groups, which contribute to the success of the conversion of PAN to AOPAN [120]. The FT-IR spectra of TiPP@AOPAN apparent not immersion a new peaks but reducing in the absorption peaks in AOPAN spectra such as reduced the peak of hydroxyl group from 3463 to 3456 cm^{-1} , the peak of CH stretching in CH, CH2 from 2933 to 2926 cm-1 , peaks corresponding to Ti-O from 442 to 419 cm-1 , while shifting the absorption peaks as C=O stretching from 1736 to 1740 cm-1 , C=O groups in primary amines (NH2) from 1628 to 1631 cm-1 , CH blending from 1446 to 1453 , and C-O stretching from 1030 to 1037 cm-1 respectively [121].

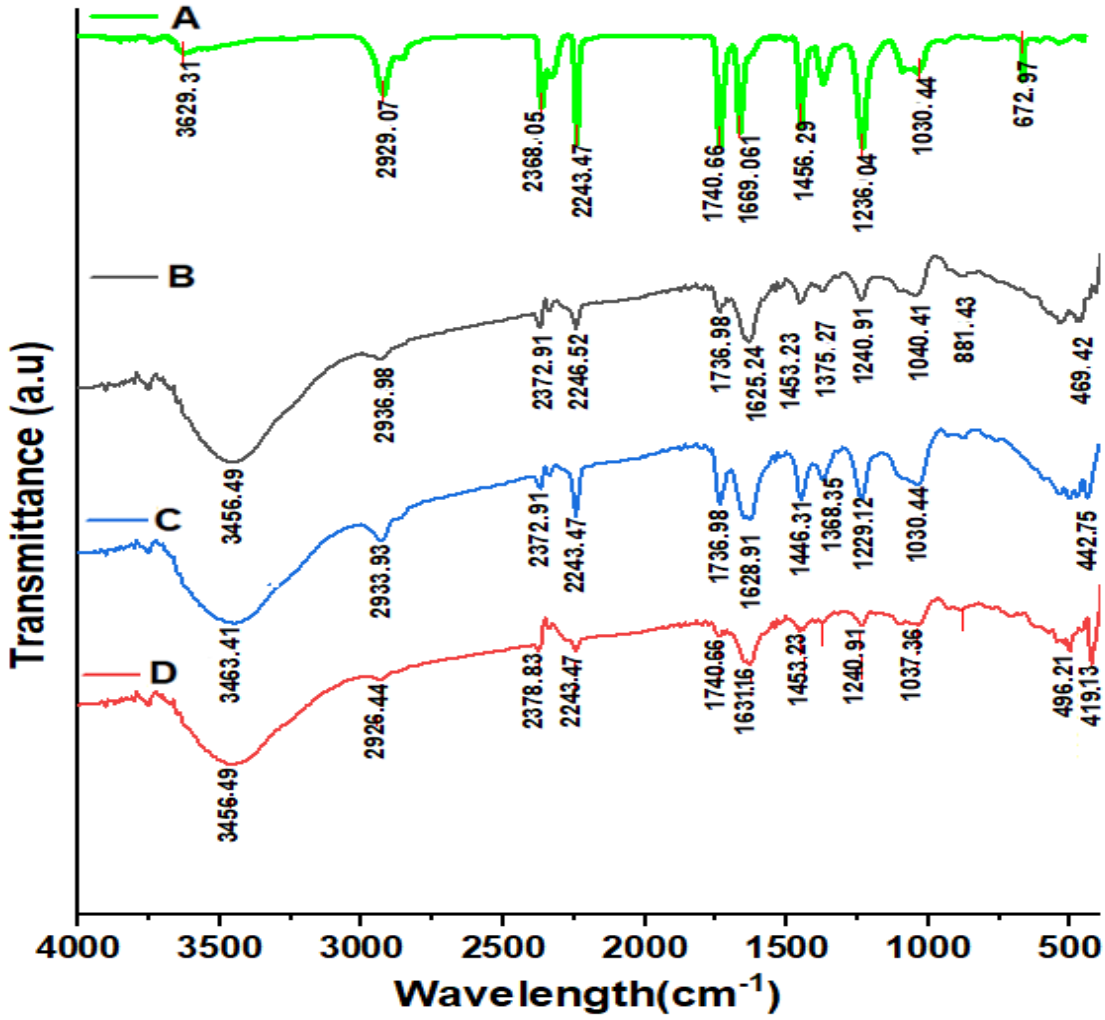

Fig. 2 FT-IR spectra of (A) pure of PAN , (B) TiPP @ PAN , (C) AOPAN , and (D) TiPP@AOPAN respectively .

4.3 XRD-analysis

Figure 3 and Table 1 show the X-ray diffraction patterns of Pure PAN, 5% TiPP @PAN and AOPAN, and 5% TiPP @AOPAN with ranges of 2 θ (10°–80°) at room temperature.

The composite nanofibers showed two strong peaks at 2 θ = 16.89° and 49.88° compared with the X-ray diffraction pattern of Pure PAN at the weaker peak at 2 θ = 24.75° depending on the d- spacing and planes hexagonal crystals 5.25 Å (100), 1.83 Å (220) for 5% TiPP @PAN sample and 3.59 Å (100) for pure PAN at Figure 4 a,d. The increment of average crystalline size and crystallinity % about 222.8 % and 38.56 % after adding 5% TiO2 to PAN respectively , this result is consistent with a previous study [122]. On the other hand, after chemical reaction between the hydroxylamine hydrochloride and PAN: DMF solution with present of sodium carbonate at 70 °C to produce the amidoxime polyacrylonitrile (AOPAN) and immersion a new bands lead to stretch vibration of C–N and C=N groups, which contribute to the success of the conversion of PAN to AOPAN. The XRD spectra of Figure 3 b (AOPAN) shows the strong peaks at 2 θ = 16.70°, 28.05°, and 52.49° according to the d- spacing and planes hexagonal crystals 5.31 Å (100), 3.10 Å (111), and 1.77 Å(221) and the composite of nanofibers at Figure 4c (5% TiPP @AOPAN) shows peaks 2 θ = 17.375°, 24.425°, and 48.475° according to the d- spacing and planes hexagonal crystals 5.13 Å (100), 3.36 Å (200) , and 1.82 Å (220) by

Increment in average crystalline size and crystallinity % about 103.87 % and 18.69 % compared with the average crystalline size and crystallinity % at 5% TiPP @PAN [123] .

Table 1 Results of XRD test

Samples	Position [°2Th.]	d-spacing [Å]	Crystalline Size [nm]	Crystallinity [%]
Pure PAN	24.75	3.59	6.8	18.80
5 % TiO2@PAN	16.89 49.88	5.25 1.83	21.95	26.05
AOPAN	16.70 28.05 52.49	5.31 3.10 1.77	44.75	30.92
5 % TiO2@AOPAN	17.375 24.425 48.475	5.13 3.36 1.82	40.00	30.34

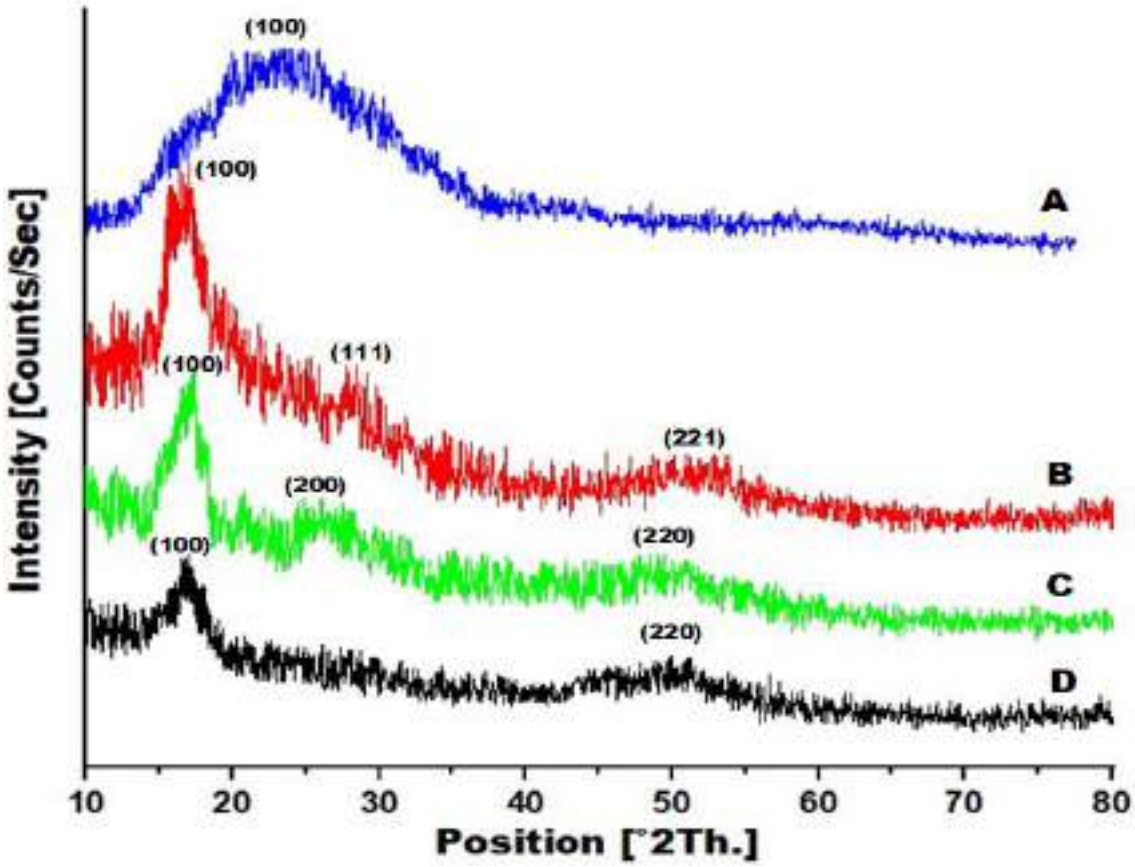
(100)
(100)
A
(100)
(111)
(221)
B
(200)
(100)
(220)
C
(220)
D
Intensity [Counts/Sec]
10
20
30
40
50
60
70
80
Position [°2Th.]

Fig.3 XRD spectra of (A) Pure PAN , (B) AOPAN , (C) 5 % TiPP@AOPAN , and (D) 5 % TiPP@PAN nanofibers

4.4 Thermal Properties

The pure nanofibers as (PAN, AOPAN) and composites nanofibers as (5 % TiPP@PAN , 5 % TiPP@AOPAN) were subjected to DSC-TGA analysis by SDT Q600 V20.9 Build 20 with range of heating temperature (0-1000°C) as shown in Figure 4. The results of the TGA analysis proved that the addition of TiPP to PAN increases the thermal stability of the composite nanofibers, due to the presence of a good interaction between them, represented by the presence of the hydroxyl group and the nitrile group, where the rate of weight loss decreased as a result of exposing the nanofibers to thermal stress by 16%, while the melting point increased from 328.32 ℃ to 366.31 ℃ and the heat required for fusion increased by 11.6 % , this results was agree with previous study [124] .On the other hand, the chemical reaction between the PAN: DMF solution and the hydroxylamine hydrochloride produced a new bands lead to stretch vibration of C–N and C=N groups because the surface of AOPAN fibers contains medoxime groups (–C (NH2) = NOH), which lead to high thermal stability [125]. Therefore, the weight loss percentage decreased by 32.53 % after chemical reaction and produced the AOPAN, also increased the meting temperature from 328.32 ℃ to 367.96 ℃ and the heat required for fusion increased by 12.1 % . In contrast, an increase in the weight loss by 9 .13 % and a decrease in the melting temperature from 366.31 ℃ to 348.37 ℃ and the heat required for fusion by 4.89 % after addition the 5 wt.% of TiPP to AOPAN compared with addition of same amount of TiPP to PAN .

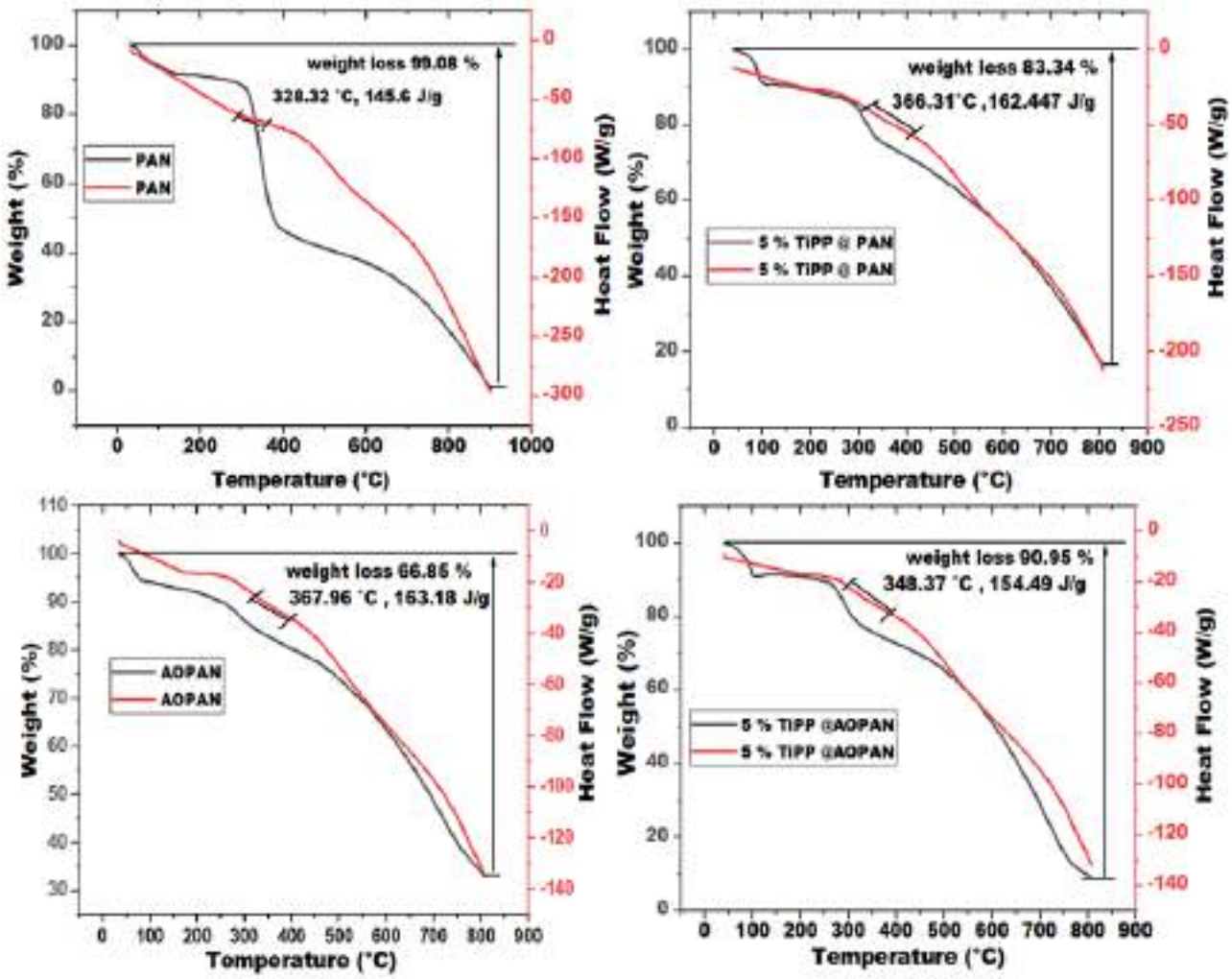

Fig. 4 DSC-TGA thermographs for pure PAN, 5 % TiPP @PAN, AOPAN, and 5 % TiPP @AOPAN respectively

Conclusion

Conclusion

Polyacrylonitrile fibers have good thermal properties and these properties improve after adding TiPP, but the development of polyacrylonitrile fibers gives better results in terms of morphological and thermal properties as well as crystallinity, so the treatment of polyacrylonitrile gives distinctive properties, especially for heavy metal ion adsorption applications and gas filtration.

References

1. P.K. Neghlani, M. Rafzadeh, F.A. Taromi, Preparation of aminated-polyacrylonitrile nanofber membranes for the adsorption of metal ions: comparison with microfbers. J. Hazard. Mater. 186(1), 182–189 (2011)

2. Habeeb SA, Hasan AS, Ţălu Ş, Jawad AJ. Enhancing the Properties of Styrene-Butadiene Rubber by Adding Borax Particles of Different Sizes. Iran. J. Chem. Chem. Eng., 2021; 40(5):1616-29.

3. J. Thilagan, S. Gopalakrishnan, T. Kannadasan, A comparative study on adsorption of copper (ii) ions in aqueous solution by; (a) chitosan blended with cellulose and cross linked by formaldehyde, (b) chitosan immobilised on red soil, (c) chitosan reinforced by banana stem fbre. Int. J. Appl. Eng. Technol. 3, 35–60 (2013)

4. Habeeb SA, Diwan AA, Albozahid MZ. A Compressive Review on Swelling Parameters and Physical Properties of Natural Rubber Nano composites. Egypt. J. Chem., 2021; 64(10):3-4.

5. T. Jiang et al., Adsorption behavior of copper ions from aqueous solution onto graphene oxide–CdS composite. Chem. Eng. J. 259, 603–610 (2015)

6. Q. Chen et al., Comparison of heavy metal removals from aqueous solutions by chemical precipitation and characteristics of precipitates. J. Water Process Eng. 26, 289–300 (2018)

7. S. A. Habeeb, L. Rajabi, and F. Dabirian, “Production of polyacrylonitrile/boehmite nanofibrous composite tubular structures by opposite-charge electrospinning with enhanced properties from a low-concentration polymer solution,” Polymer Composites, vol. 41, no. 4, pp. 1649–1661, 2020

8. A.P. de los Ríos et al., Removal of metal ions from aqueous solutions by extraction with ionic liquids. J. Chem. Eng. Data 55(2), 605–608 (2010

9. Habeeb SA, Alobad ZK, Albozahid MA. Effect of zinc oxide loading levels on the cure characteristics, mechanical and aging properties of the epdm rubber. Int. J. Mech. Eng., 2019;10 (1):133-41.

10. K. Saeed et al., Preparation of amidoxime-modifed polyacrylonitrile (PAN-oxime) nanofbers and their applications to metal ions adsorption. J. Membr. Sci. 322(2), 400–405 (2008)

11. Habeeb SA, Alobad ZK, Albozahid MA. The Effecting of Physical Properties of Inorganic Fillers on Swelling Rate of Rubber Compound: A review Study. J. Univ. Babylon eng. sci., 2019; 27(1):94-104.

12. A. Mahapatra, B.G. Mishra, G. Hota, Electrospun Fe2O3–Al2O3 nanocomposite fbers as efcient adsorbent for removal of heavy metal ions from aqueous solution. J. Hazard. Mater. 258–259, 116–123 (2013)

13. S. A. Habeeb, “Impact of polymeric solutions parameters on morphological properties of composite nanofibers,” Journal of University of Babylon for Engineering Sciences, vol. 29, no. 2, pp. 115–120, 2021.

14. D. Faris, N. J. Hadi, and S. A. Habeeb, “Effect of rheological properties of (poly vinyl alcohol/dextrin/naproxen) emulsion on the performance of drug encapsulated nanofibers,” Materials Today: Proceedings, vol. 42, pp. 2725–2732, 2021

15. D. Yang et al., Functionalized chitosan electrospun nanofber membranes for heavy-metal removal. Polymer 163, 74–85 (2019)

16. S. Habeeb, L. Rajabi, and F. Dabirian,“Comparing two electrospinning methods in producing polyacrylonitrile nanofibrous tubular structures with enhanced properties,” Iranian journal of chemistry and chemical engineering, vol. 38, no. 3, pp. 23– 42, 2019

17. S.K. Nataraj, K.S. Yang, T.M. Aminabhavi, Polyacrylonitrilebased nanofbers: a state-of-the-art review. Prog. Polym. Sci. 37(3), 487–513 (2012)

18. B. A. Nadhim and S. A. Habeeb, “Studying the physical properties of non-woven polyacrylonitrile nanofibers after adding γ-Fe2O3 nanoparticles,” Egyptian Journal of Chemistry, vol. 64, no. 12, pp. 7521–7530, 2021.

19. S. A. Habeeb and B. A. Nadhim, “Removal of nickel (II) ions, low level pollutants, and total bacterial colony count from wastewater by composite nanofibers film,” Scientia Iranica, 2022, http://scientiairanica.sharif.edu/article_22970.html.

20. B. Zhang et al., Synergistic nanofbrous adsorbent for uranium extraction from seawater. RSC Adv. 6(85), 81995–82005 (2016)

21. M. K. Abdulkadhim and S. A. Habeeb, “The possibility of producing uniform nanofibers from blends of natural biopolymers,” Materials Performance and Characterization, vol. 11, no. 1, pp. 20220045–20220323, 2022

22. Gupta, A. K.; Paliwal, D. K.; Bajaj, P. (1998). "Melting behavior of acrylonitrile polymers". Journal of Applied Polymer Science. 70 (13): 2703–2709. doi:10.1002/(sici)1097-4628(19981226)70:13<2703::aid-app15>3.3.co;2-u

23. Delong, Liu (2011). "Synthesis of Polyacrylonitrile by Single-electron Transfer-living Radical Polymerization Using Fe(0) as Catalyst and Its Absorption Properties After Modification". Journal of Polymer Science Part A: Polymer Chemistry. 49 (13): 2916–2923. Bibcode:2011JPoSA..49.2916L. doi:10.1002/pola.24727.

24. "Polyacrylonitrile (PAN) Carbon Fibers Industrial Capability Assessment" (PDF). United States of America Department of Defense. Archived from the original (PDF) on 4 March 2016. Retrieved 4 December 2013.

25. "Top 9 Things You Didn't Know about Carbon Fiber | Department of Energy". Energy.gov. 2013-03-29. Retrieved 2013-12-08.

26. John McElroy. "Manufacturing advances bring carbon fiber closer to mass production". Autoblog. Retrieved 2013-12-08.

27. Handbook of Electrochemistry. Elsevier. 2021-07-02.

28. Alistair Holdsworth. "The Effect of Gamma Irradiation on the Ion Exchange Properties of Caesium-Selective Ammonium Phosphomolybdate Polyacrylonitrile (AMP-PAN) Composites under Spent Fuel Recycling Conditions". MDPI. Retrieved 2021-02-03.

29. Nna-Mvondo, Delphine; de la Fuente, José L.; Ruiz-Bermejo, Marta; Khare, Bishun; McKay, Christopher P. (September 2013). "Thermal characterization of Titan's tholins by simultaneous TG–MS, DTA, DSC analysis". Planetary and Space Science. 85: 279–288. Bibcode:2013P&SS...85..279N. doi:10.1016/j.pss.2013.06.025.

30. Fukushima, R.S.; Dehority, B.A.; Loerch, S.C. (1 January 1991). "Modification of a colorimetric analysis for lignin and its use in studying the inhibitory effects of lignin on forage digestion by ruminal microorganisms". J. Anim. Sci. 69 (1): 295–304. doi:10.2527/1991.691295x. PMID 2005024. Archived from the original on 10 October 2008.4

31. Elstner, E.F.; Heupel, A. (February 1976). "Inhibition of nitrite formation from hydroxylammoniumchloride: a simple assay for superoxide dismutase". Anal. Biochem. 70 (2): 616–20. doi:10.1016/0003-2697(76)90488-7. PMID 817618.

32 . Jump up to:a b c d Harper, J. P. (1936). Antipov, Evgeny; Bismayer, Ulrich; Huppertz, Hubert; Petrícek, Václav; Pöttgen, Rainer; Schmahl, Wolfgang; Tiekink, E. R. T.; Zou, Xiaodong (eds.). "Crystal Structure of Sodium Carbonate Monohydrate, Na2CO3. H2O". Zeitschrift für

Kristallographie - Crystalline Materials. 95 (1): 266–273. doi:10.1524/zkri.1936.95.1.266. ISSN 2196-7105. Retrieved 2014-07-25.

33. Jump up to:a b c d e f g Lide, David R., ed. (2009). CRC Handbook of Chemistry and Physics (90th ed.). Boca Raton, Florida: CRC Press. ISBN 978-1-4200-9084-0.

34. Jump up to:a b Seidell, Atherton; Linke, William F. (1919). Solubilities of Inorganic and Organic Compounds (2nd ed.). New York: D. Van Nostrand Company. p. 633.

35. Jump up to:a b Comey, Arthur Messinger; Hahn, Dorothy A. (February 1921). A Dictionary of Chemical Solubilities: Inorganic (2nd ed.). New York: The MacMillan Company. pp. 208–209.

36. Jump up to:a b c d Anatolievich, Kiper Ruslan. "sodium carbonate". chemister.ru. Retrieved 2014-07-25.

37. "Sodium carbonate". www.chemicalbook.com. Retrieved 25 June 2021.

38. Jump up to:a b c Pradyot, Patnaik (2003). Handbook of Inorganic Chemicals. McGraw-Hill. p. 861. ISBN 978-0-07-049439-8.

39. "minerals.usgs.gov/minerals" (PDF). United States Geographical Survey.

40. Christian Thieme (2000). "Sodium Carbonates". Ullmann's Encyclopedia of Industrial Chemistry. Weinheim: Wiley-VCH. doi:10.1002/14356007.a24_299. ISBN 978-3527306732.

41. Jump up to:a b c https://www.ccmr.cornell.edu/wp-content/uploads/sites/2/2015/11/Water-Hardness-Reading.pdf[bare URL PDF]

42. Jump up to:a b McGee, Harold (24 September 2010). "For Old-Fashioned Flavor, Bake the Baking Soda". The New York Times. Retrieved 25 April 2019.

43. "Sodium Carbonate". corrosionpedia. Janalta Interactive. Retrieved 9 November 2020.

44. "Hazardous Substances Data Bank (HSDB) - N,N-DIMETHYLFORMAMIDE".

45. Bipp, H.; Kieczka, H. "Formamides". Ullmann's Encyclopedia of Industrial Chemistry. Weinheim: Wiley-VCH. doi:10.1002/14356007.a12_001.pub2.

46. Vilsmeier, Anton; Haack, Albrecht (1927). "Über die Einwirkung von Halogenphosphor auf Alkyl-formanilide. Eine neue Methode zur Darstellung sekundärer und tertiärer p-Alkylamino-benzaldehyde" [On the reaction of phosphorus halides with alkyl formanilides. A new method for the preparation of secondary and tertiary p-alkylamino-benzaldehyde]. Ber. Dtsch. Chem. Ges. A/B (in German). 60 (1): 119–122. doi:10.1002/cber.19270600118.

47. Meth-Cohn, Otto; Stanforth, Stephen P. (1993). "The Vilsmeier-Haack Reaction". In Trost, Barry M.; Heathcock, Clayton H. (eds.). Additions to CX π-Bonds, Part 2. Comprehensive Organic Synthesis: Selectivity, Strategy and Efficiency in Modern Organic Chemistry. Vol. 2. Elsevier. pp. 777–794. doi:10.1016/B978-0-08-052349-1.00049-4. ISBN 9780080405933.

48. Bouveault, Louis (1904). "Modes de formation et de préparation des aldéhydes saturées de la série grasse" [Methods of preparation of saturated

aldehydes of the aliphatic series]. Bulletin de la Société Chimique de Paris. 3rd series (in French). 31: 1306–1322.

49. Bouveault, Louis (1904). "Nouvelle méthode générale synthétique de préparation des aldéhydes" [Novel general synthetic method for preparing aldehydes]. Bulletin de la Société Chimique de Paris. 3rd series (in French). 31: 1322–1327.

50. Li, Jie Jack (2014). "Bouveault aldehyde synthesis". Name Reactions: A Collection of Detailed Mechanisms and Synthetic Applications (5th ed.). Springer Science & Business Media. pp. 72–73. ISBN 978-3-319-03979-4.

51. Oestreich, Martin, ed. (2009). The Mizoroki–Heck Reaction. John Wiley & Sons. ISBN 9780470716069.

52. Clayden, J. (2001). Organic Chemistry. Oxford: Oxford University Press. pp. 276–296. ISBN 0-19-850346-6.

53. Ansell, M. F. in "The Chemistry of Acyl Halides"; S. Patai, Ed.; John Wiley and Sons: London, 1972; pp 35–68.

54. Haddon, R.; Itkis, M. (March 2008). "3. Near-Infrared (NIR) Spectroscopy" (pdf). In Freiman, S.; Hooker, S.; Migler; K.; Arepalli, S. (eds.). Publication 960-19 Measurement Issues in Single Wall Carbon Nanotubes. NIST. p. 20. Retrieved 2012-06-28.

55. Ziabicki, A. (1976) Fundamentals of fiber formation, John Wiley and Sons, London, ISBN 0-471-98220-2.

56. High speed video of the taylor cone formation and electrospinning. youtube.com

57. Single nozzle electrospinning process nanofiber formation video. youtube.com

58. High speed video of the whipping instability. youtube.com

59. Jump up to:a b c Li D, Xia Y (2004). "Electrospinning of Nanofibers: Reinventing the Wheel?". Advanced Materials. 16 (14): 1151–1170. Bibcode:2004AdM....16.1151L. doi:10.1002/adma.200400719. S2CID 137659394.

60. Merritt SR, Exner AA, Lee Z, von Recum HA (May 2012). "Electrospinning and Imaging". Advanced Engineering Materials. 14 (5): B266–B278. doi:10.1002/adem.201180010. S2CID 136486578.

61. ^Sivan, Manikandan; Madheswaran, Divyabharathi; Valtera, Jan; Kostakova, Eva Kuzelova; Lukas, David (1 January 2022). "Alternating current electrospinning: The impacts of various high-voltage signal shapes and frequencies on the spinnability and productivity of polycaprolactone nanofibers". Materials & Design. 213: 110308. doi:10.1016/j.matdes.2021.110308. ISSN 0264-1275. S2CID 245075252.

62. Balogh A, Cselkó R, Démuth B, Verreck G, Mensch J, Marosi G, Nagy ZK (November 2015). "Alternating current electrospinning for preparation of fibrous drug delivery systems". International Journal of Pharmaceutics. 495 (1): 75–80. doi:10.1016/j.ijpharm.2015.08.069. PMID 26320549.

63. Sivan M, Madheswaran D, Asadian M, Cools P, Thukkaram M, Van Der Voort P, et al. (15 October 2020). "Plasma treatment effects on bulk properties of polycaprolactone nanofibrous mats fabricated by uncommon AC electrospinning: A comparative study". Surface and Coatings Technology. 399: 126203. doi:10.1016/j.surfcoat.2020.126203. ISSN 0257-8972. S2CID 224924026.

64. Manikandan S, Divyabharathi M, Tomas K, Pavel P, David L (1 January 2019). "Production of poly (ε-caprolactone) Antimicrobial Nanofibers by Needleless Alternating Current Electrospinning". Materials Today: Proceedings. 6th International Conference on Recent Advances in Materials, Minerals & Environment (RAMM) 2018, RAMM 2018, 27–29 November 2018, Penang, Malaysia. 17: 1100–1104. doi:10.1016/j.matpr.2019.06.526. ISSN 2214-7853. S2CID 202207593.

65. Lawson C, Stanishevsky A, Sivan M, Pokorny P, Lukáš D (2016). "Rapid fabrication of poly(ε-caprolactone) nanofibers using needleless alternating current electrospinning". Journal of Applied Polymer Science. 133 (13): n/a. doi:10.1002/app.43232. ISSN 1097-4628.

66. Madheswaran, Divyabharathi; Sivan, Manikandan; Valtera, Jan; Kostakova, Eva Kuzelova; Egghe, Tim; Asadian, Mahtab; Novotny, Vit; Nguyen, Nhung H. A.; Sevcu, Alena; Morent, Rino; Geyter, Nathalie De (2022). "Composite yarns with antibacterial nanofibrous sheaths produced by collectorless alternating-current electrospinning for suture applications". Journal of Applied Polymer Science. 139 (13): 51851. doi:10.1002/app.51851. ISSN 1097-4628. S2CID 243969095.

67. Niu, Haitao; Lin, Tong (2012). "Fiber generators in needleless electrospinning". Journal of Nanomaterials. 12.

68. Keirouz A, Zakharova M, Kwon J, Robert C, Koutsos V, Callanan A, et al. (July 2020). "High-throughput production of silk fibroin-based electrospun fibers as biomaterial for skin tissue engineering applications". Materials Science & Engineering. C, Materials for Biological Applications. 112: 110939. doi:10.1016/j.msec.2020.110939. hdl:20.500.11820/62973e7f-cb3d-4064-895b-d9e83458e062. PMID 32409085. S2CID 216267121.

69. Varesano, A.; Carletto, R.A.; Mazzuchetti, G. (2009). "Experimental investigations on the multi-jet electrospinning process". Journal of Materials Processing Technology. 209 (11): 5178–5185. doi:10.1016/j.jmatprotec.2009.03.003.

70. Jump up to:a b Waqas, Muhammad; Keirouz, Antonios; Sanira Putri, Maria Kana; Fazal, Faraz; Diaz Sanchez, Francisco Javier; Ray, Dipa; Koutsos, Vasileios; Radacsi, Norbert (1 June 2021). "Design and development of a nozzle-free electrospinning device for the high-throughput production of biomaterial nanofibers". Medical Engineering & Physics. 92: 80–87. doi:10.1016/j.medengphy.2021.04.007. hdl:20.500.11820/9616f724-7850-47da-895b-75c9d06d149b. ISSN 1350-4533. PMID 34167715. S2CID 235543210.

71. Liu, Y.; He, J.-H.; Yu, J.-Y. (2008). "Bubble-electrospinning: a novel method for making nanofibers". Journal of Physics: Conference Series. 96

(1): 012001. Bibcode:2008JPhCS..96a2001L. doi:10.1088/1742-6596/96/1/012001.

72. Nagy ZK, Balogh A, Démuth B, Pataki H, Vigh T, Szabó B, et al. (March 2015). "High speed electrospinning for scaled-up production of amorphous solid dispersion of itraconazole". International Journal of Pharmaceutics. 480 (1–2): 137–42. doi:10.1016/j.ijpharm.2015.01.025. PMID 25596415.

73. Thoppey, N.M.; Bochinski, J.R.; Clarke, L.I.; Gorga, R.E. (2010). "Unconfined fluid electrospun into high quality nanofibers from a plate edge" (PDF). Polymer. 51 (21): 4928–4936. doi:10.1016/j.polymer.2010.07.046.

74. Thoppey NM, Bochinski JR, Clarke LI, Gorga RE (August 2011). "Edge electrospinning for high throughput production of quality nanofibers". Nanotechnology. 22 (34): 345301. Bibcode:2011Nanot..22H5301T. doi:10.1088/0957-4484/22/34/345301. PMID 21799242. S2CID 54921.

75. Varabhas, J.; Chase, G.; Reneker, D. (2008). "Electrospun nanofibers from a porous hollow tube". Polymer. 49 (19): 4226–4229. doi:10.1016/j.polymer.2008.07.043.

76. Lu B, Wang Y, Liu Y, Duan H, Zhou J, Zhang Z, et al. (August 2010). "Superhigh-throughput needleless electrospinning using a rotary cone as spinneret". Small. 6 (15): 1612–6. doi:10.1002/smll.201000454. PMID 20602427.

78. Lee JH, Shin DW, Nam KB, Gim YH, Ko HS, Seo DK, Lee GH, Kim YH, Kim SW, Oh TS, Yoo JB (2016). "Continuous bundles of aligned electrospun PAN nano-fiber using electrostatic spiral collector and converging coil". Polymer. 84 (10): 52–58. doi:10.1016/j.polymer.2015.11.046.

79. Balogh A, Horváthová T, Fülöp Z, Loftsson T, Harasztos AH, Marosi G, Nagy ZK (April 2015). "Electroblowing and electrospinning of fibrous diclofenac sodium-cyclodextrin complex-based reconstitution injection". Journal of Drug Delivery Science and Technology. 26: 28–34. doi:10.1016/j.jddst.2015.02.003.

80. Jump up to:a b Nagy ZK, Balogh A, Drávavölgyi G, Ferguson J, Pataki H, Vajna B, Marosi G (February 2013). "Solvent-free melt electrospinning for preparation of fast dissolving drug delivery system and comparison with solvent-based electrospun and melt extruded systems". Journal of Pharmaceutical Sciences. 102 (2): 508–17. doi:10.1002/jps.23374. PMID 23161110.

81. Filatov Y, Budyka A, Kirichenko V (2007). Electrospinning of micro- and nanofibers : fundamentals and applications in separation and filtration processes. Translated by Letterman D. New York: Begell House. ISBN 978-1-56700-241-6.

82. Ajayan P. M., Schadler, L. S. and Braun, P. V. (2003) Nanocomposite Science and Technology, Weinheim, Wiley-VCH, ISBN 9783527602124, doi:10.1002/3527602127.

83. Donaldson Nanofiber Products Archived 2011-07-10 at the Wayback Machine

84. Subbiah T, Bhat GS, Tock RW, Parameswaran S, Ramkumar SS (2005). "Electrospinning of nanofibers". Journal of Applied Polymer Science. 96 (2): 557–569. doi:10.1002/app.21481.

85. Lee S, Obendorf SK (2007). "Use of Electrospun Nanofiber Web for Protective Textile Materials as Barriers to Liquid Penetration". Textile Research Journal. 77 (9): 696–702. doi:10.1177/0040517507080284. S2CID 136722801.

86. Yu-Jun Zhang; Yu-Dong Huang (2004). "Electrospun non-woven mats of EVOH". XXIst International Symposium on Discharges and Electrical

Insulation in Vacuum, 2004. Proceedings. ISDEIV. Vol. 1. p. 106. doi:10.1109/DEIV.2004.1418615. ISBN 0-7803-8461-X.

87. Sill TJ, von Recum HA (May 2008). "Electrospinning: applications in drug delivery and tissue engineering". Biomaterials. 29 (13): 1989–2006. doi:10.1016/j.biomaterials.2008.01.011. PMID 18281090.

88. Li WJ, Laurencin CT, Caterson EJ, Tuan RS, Ko FK (June 2002). "Electrospun nanofibrous structure: a novel scaffold for tissue engineering". Journal of Biomedical Materials Research. 60 (4): 613–21. doi:10.1002/jbm.10167. PMID 11948520. S2CID 1047910.

89. Jaberifard, Farnaz; Ramezani, Soghra; Ghorbani, Marjan; Arsalani, Nasser; Mortazavi Moghadam, Fatemeh (January 2023). "Investigation of wound healing efficiency of multifunctional eudragit/soy protein isolate electrospun nanofiber incorporated with ZnO loaded halloysite nanotubes and allantoin". International Journal of Pharmaceutics. 630: 122434. doi:10.1016/j.ijpharm.2022.122434. PMID 36435502. S2CID 253958743.

90. Doustdar, Fatemeh; Ramezani, Soghra; Ghorbani, Marjan; Mortazavi Moghadam, Fatemeh (November 2022). "Optimization and characterization of a novel tea tree oil-integrated poly (ε-caprolactone)/soy protein isolate electrospun mat as a wound care system". International Journal of

Pharmaceutics. 627: 122218. doi:10.1016/j.ijpharm.2022.122218. PMID 36155796. S2CID 252500879.

91. Khil MS, Cha DI, Kim HY, Kim IS, Bhattarai N (November 2003). "Electrospun nanofibrous polyurethane membrane as wound dressing". Journal of Biomedical Materials Research Part B: Applied Biomaterials. 67 (2): 675–9. doi:10.1002/jbm.b.10058. PMID 14598393.

92. Weldon CB, Tsui JH, Shankarappa SA, Nguyen VT, Ma M, Anderson DG, Kohane DS (August 2012). "Electrospun drug-eluting sutures for local anesthesia". Journal of Controlled Release. 161 (3): 903–9. doi:10.1016/j.jconrel.2012.05.021. hdl:1721.1/101125. PMC 3412890. PMID 22609349.

93. Andukuri A, Kushwaha M, Tambralli A, Anderson JM, Dean DR, Berry JL, et al. (January 2011). "A hybrid biomimetic nanomatrix composed of electrospun polycaprolactone and bioactive peptide amphiphiles for cardiovascular implants". Acta Biomaterialia. 7 (1): 225–33. doi:10.1016/j.actbio.2010.08.013. PMC 2967669. PMID 20728588.

94. Taepaiboon P, Rungsardthong U, Supaphol P (September 2007). "Vitamin-loaded electrospun cellulose acetate nanofiber mats as transdermal and dermal therapeutic agents of vitamin A acid and vitamin E". European

Journal of Pharmaceutics and Biopharmaceutics. 67 (2): 387–97. doi:10.1016/j.ejpb.2007.03.018. PMID 17498935.

95. Nagy ZK, Nyúl K, Wagner I, Molnár K, Marosi G (2010). "Electrospun water soluble polymer mat for ultrafast release of Donepezil HCl" (PDF). Express Polymer Letters. 4 (12): 763–772. doi:10.3144/expresspolymlett.2010.92.

96. Di Gesù R, Amato G, Gottardi R (October 2019). "Electrospun Scaffolds in Tendons Regeneration: a review". Muscles, Ligaments and Tendons Journal. 9 (4): 478–493. doi:10.32098/mltj.04.2019.02.

97. Di Gesù R, Merlettini A, Gualandi C, Focarete ML (January 2018). "Advances in multidrug delivery from electrospun nanomaterials". InCore-Shell Nanostructures for Drug Delivery and Theranostics. Woodhead Publishing. pp. 405–430. doi:10.1016/B978-0-08-102198-9.00014-4. ISBN 978-0-08-102198-9.

98. Dolci LS, Perone RC, Di Gesù R, Kurakula M, Gualandi C, Zironi E, et al. (June 2021). "Design and In Vitro Study of a Dual Drug-Loaded Delivery System Produced by Electrospinning for the Treatment of Acute Injuries of the Central Nervous System". Pharmaceutics. 13 (6): 848. doi:10.3390/pharmaceutics13060848. PMC 8227370. PMID 34201089.

99. Zealand BK, Lepe P, Hosie IC. "A New Spin on Delivery: Electrospun Collagen Drives Actives to New Depths". Cosmetics & Toiletries. New Revolution Fibres Ltd. Retrieved 31 August 2019.

71^ Balogh A, Domokos A, Farkas B, Farkas A, Rapi Z, Kiss D, et al. (October 2018). "Continuous end-to-end production of solid drug dosage forms: Coupling flow synthesis and formulation by electrospinning" (PDF). Chemical Engineering Journal. 350: 290–299. doi:10.1016/j.cej.2018.05.188.

100. Molnar K, Vas LM, Czigany T (2011). "Determination of tensile strength of electrospun single nanofibers through modeling tensile behavior of the nanofibrous mat". Composites Part B: Engineering. 43: 15–21. doi:10.1016/j.compositesb.2011.04.024.

101. Siddiqui N, Kishori B, Rao S, Anjum M, Hemanth V, Das S, Jabbari E (2021). "Electropsun Polycaprolactone Fibres in Bone Tissue Engineering: A Review". Molecular Biotechnology. 63 (5): 363–388. doi:10.1007/s12033-021-00311-0. PMID 33689142. S2CID 232164709.

102. Poshina DN, Tyshkunova IV, Petrova VA, Skorik YA (2021). "Electrospinning of Polysaccharides for Tissue Engineering Applications".

Reviews and Advances in Chemistry. 11 (1–2): 112–133. doi:10.1134/S2079978021010052. S2CID 237539377.

103. Matthews JA, Wnek GE, Simpson DG, Bowlin GL (2002). "Electrospinning of collagen nanofibers". Biomacromolecules. 3 (2): 232–8. doi:10.1021/bm015533u. PMID 11888306.

104. "Revolution Fibres is manufacturing to the sun and back". techweek.co.nz. Retrieved 31 August 2019.

105. "Electrospinning Mass Production Machine Providers". electrospintech.com. Retrieved 15 January 2016.

106. "Resonant X-ray Scattering | Shen Laboratory". arpes.stanford.edu. Retrieved 2019-07-10.

Kepler J (1611). Strena seu de Nive Sexangula. Frankfurt: G. Tampach. ISBN 3-321-00021-0.

Steno N (1669). De solido intra solidum naturaliter contento dissertationis prodromus. Florentiae.

Hessel JF (1831). Kristallometrie oder Kristallonomie und Kristallographie. Leipzig.

Bravais A (1850). "Mémoire sur les systèmes formés par des points distribués regulièrement sur un plan ou dans l'espace". Journal de l'École Polytechnique. 19: 1

107. HTTPS://PHOTOMETRICS.NET/FIELD-EMISSION-SCANNING-ELECTRON-MICROSCOPY-FESEM/

108. HTTPS://PHOTOMETRICS.NET/DIFFERENTIAL-SCANNING-CALORIMETRY-DSC/

109. HTTPS://PHOTOMETRICS.NET/THERMOGRAVIMETRIC-ANALYSIS-TGA/

110. HTTPS://PHOTOMETRICS.NET/FOURIER-TRANSFORM-INFRARED-FTIR-SPECTROSCOPY/

INTERNATIONAL CONFERENCE ON RECENT ADVANCES IN MATERIALS, MINERALS & ENVIRONMENT (RAMM) 2018, RAMM 2018, 27–29 NOVEMBER 2018, PENANG, MALAYSIA. 17: 1100–1104. DOI:10.1016/J.MATPR.2019.06.526. ISSN 2214-7853. S2CID 202207593.

111. Corbari, L; et al. (2008). "Iron oxide deposits associated with the ectosymbiotic bacteria in the hydrothermal vent shrimp Rimicaris exoculata". Biogeosciences. 5 (5): 1295–1310. Bibcode:2008BGeo....5.1295C. doi:10.5194/bg-5-1295-2008.

Joseph Goldstein (2003). Scanning Electron Microscopy and X-Ray Microanalysis. Springer. ISBN 978-0-306-47292-3. Retrieved 26 May 2012.

Jenkins, R. A.; De Vries, J. L. (1982). Practical X-Ray Spectrometry. Springer. ISBN 978-1-468-46282-1.

Kosasih, Felix Utama; Cacovich, Stefania; Divitini, Giorgio; Ducati, Caterina (17 November 2020). "Nanometric Chemical Analysis of Beam-Sensitive Materials: A Case

Study of STEM-EDX on Perovskite Solar Cells". Small Methods. 5 (2): 2000835. doi:10.1002/smtd.202000835. PMID 34927887.

112. https://www.ahelite.com/Polyacrylonitrile-PAN-Fiber-pd138524.html

113. https://www.sigmaaldrich.com/IQ/en/product/mm/hx0770

114. https://www.etisoda.com/en/sodium-carbonate-dense-soda-ash/

115. Mohammed, Y. A., Ma, F., Liu, L., Zhang, C., Dong, H., Wang, Q., ... & Al-Wahbi, A. A. (2021). Preparation of electrospun polyvinylidene fluoride/amidoximized polyacrylonitrile nanofibers for trace metal ions removal from contaminated water. Journal of Porous Materials, 28, 383-392

116. Saeed, K., Haider, S., Oh, T. J., & Park, S. Y. (2008). Preparation of amidoxime-modified polyacrylonitrile (PAN-oxime) nanofibers and their applications to metal ions adsorption. Journal of Membrane Science, 322(2), 400-405.

117. Xiao, L., Xu, J., Liu, X., Zhang, Y., Zhang, B., Yao, J., ... & Pan, X. (2016). Mesoporous TiO2 nanowire film for dye-sensitized solar cell. Journal of Nanoscience and Nanotechnology, 16(6), 5605-5610.

118. Zhang, X., Pan, J. H., Du, A. J., Xu, S., & Sun, D. D. (2009). Room-temperature fabrication of anatase TiO2 submicrospheres with nanothornlike shell for photocatalytic degradation of methylene blue. Journal of Photochemistry and Photobiology A: Chemistry, 204(2-3), 154-160.

119. Ejraei, A., Aroon, M. A., & Saravani, A. Z. (2019). Wastewater treatment using a hybrid system combining adsorption, photocatalytic degradation and membrane filtration processes. Journal of Water Process Engineering, 28, 45-53.

120. Mohammed, Y. A., Ma, F., Liu, L., Zhang, C., Dong, H., Wang, Q., ... & Al-Wahbi, A. A. (2021). Preparation of electrospun polyvinylidene

fluoride/amidoximized polyacrylonitrile nanofibers for trace metal ions removal from contaminated water. Journal of Porous Materials, 28, 383-392

121. Chaúque, E. F., Adelodun, A. A., Dlamini, L. N., Greyling, C. J., Ray, S. C., & Ngila, J. C. (2017). Synthesis and photocatalytic application of TiO2 nanoparticles immobilized on polyacrylonitrile nanofibers using EDTA chelating agents. Materials Chemistry and Physics, 192, 108-124.

122. Khalil, K. A., Eltaleb, H., Abdo, H. S., Al-Deyab, S. S., & Fouad, H. (2014). Carbon nanofibers containing Ag/TiO2 composites as a preliminary stage for CDI Technology. Journal of Materials Science and Chemical Engineering, 2(01), 31-37

123. Mehrpouya, F., Tavanai, H., Morshed, M., & Ghiaci, M. (2012). The formation of titanium dioxide crystallite nanoparticles during activation of PAN nanofibers containing titanium isopropoxide. Journal of Nanoparticle Research, 14, 1-11

124. Chaúque, E. F., Adelodun, A. A., Dlamini, L. N., Greyling, C. J., Ray, S. C., & Ngila, J. C. (2017). Synthesis and photocatalytic application of TiO2 nanoparticles immobilized on polyacrylonitrile nanofibers using EDTA chelating agents. Materials Chemistry and Physics, 192, 108-124

125. Wu, D., Feng, Q., Xu, T., Wei, A., & Fong, H. (2018). Electrospun blend nanofiber membrane consisting of polyurethane, amidoxime polyarcylonitrile, and β-cyclodextrin as high-performance carrier/support for efficient and reusable immobilization of laccase. Chemical Engineering Journal, 331, 517-526